# Petrology of Avachites, High-Magnesian Basalts of Avachinsky Volcano, Kamchatka: I. General Characteristics and Composition of Rocks and Minerals

**M. V. Portnyagin\*,\*\*,\*\*\*, P. Yu. Plechov\*\*\*\*, S. V. Matveev\*\*\*\*\*,**
**A. B. Osipenko\*\*\*\*\*\*, and N. L. Mironov\*\***

*\*IfM-GEOMAR, Division of the Ocean Floor,*
*Wischhofstr. 1–3, Kiel, 24148 Germany*
*e-mail: mportnyagin@ifm-geomar.de*
*\*\*Vernadsky Institute of Geochemistry and Analytical Chemistry (GEOKhI),*
*Russian Academy of Sciences, ul. Kosygina 19, Moscow, 119991 Russia*
*\*\*\*Institute of Volcanology and Seismology, Far East Division, Russian Academy of Sciences,*
*bul'v. Piipa 9, Petropavlosk-Kamchatskii, 683006 Russia*
*\*\*\*\*Faculty of Geology, Moscow State University,*
*Vorob'evy gory, Moscow, 119899 Russia*
*\*\*\*\*\*University of Alberta, 1-26 Earth Sciences Building,*
*Edmonton, Alberta, Canada*
*\*\*\*\*\*\*Vernadsky State Geological Museum, Russian Academy of Sciences,*
*ul. Mokhovaya 11/2, Moscow, 103009 Russia*
Received June 10, 2003

**Abstract**—In 1935, A.N. Zavaritskii described high-magnesian [MgO/(MgO + FeO\*) = 0.73–0.82] basalts and picrites, which are unique in Kamchatka and were found on Avachinsky volcano and eventually named avachites. This paper systematizes data on the composition of these rocks and presents the results of their detailed mineralogical examination on an electron microprobe (EMPA) and with the use of secondary-ion mass spectrometry (SIMS) and vibrational IR spectrometry. The results thus obtained suggest that avachites are of volcanic genesis and were produced by the crystallization of olivine ($Fo_{91-80}$), clinopyroxene (Mg# = 92.5–73 mol %), and spinel [Mg# = 18–59 mol %, Cr/(Cr + Al) = 0.82–0.55] from a basaltic ($SiO_2 \leq 52$ wt %, MgO ~ 13 wt %) parental melt, whose composition was intermediate between those of island-arc ankaramites and high-Ca boninites. The high-Mg chemistry of the rocks (MgO = 14–20 wt %) is explained by the accumulation of olivine and pyroxene phenocrysts in an evolved basaltic melt (MgO ~ 5 wt %), which composes groundmass of avachites. The minerals crystallized under pressures of 1.0–0.1 GPa, at temperatures of $\leq 1380-1050°C$, and an oxygen fugacity of $\Delta QFM = 0.5-2.0$. The results of the IR spectroscopy of the olivine suggest that the parental magmas contained $\geq 0.5$ wt % $H_2O$. The parental magmas of avachites were derived at high degrees (>20%) of the partial melting of a mantle source that was depleted more strongly than the source of mid-oceanic ridge basalts (MORB) and was metasomatized by a fluid or melt rich in LREE, Th, Ba, K, and Sr. The typical basaltic andesites of Avachinsky volcano can be genetically related to avachites and could be produced by olivine and pyroxene crystallization from parental melts of similar composition but under pressures varying within a narrower range. The composition of the associated primitive basalts indicates that the parental melts of the volcano were heterogeneous, and magmas of ankaramite composition could contribute to the genesis of volcanic series in Kamchatka.

## INTRODUCTION

Volcanism at island arcs and active continental margins is related to the partial melting of ultramafic material in mantle wedges above subduction zones (see, for example, Gill, 1981). At the same time, it has been long known that arc lavas are of predominantly andesite composition. Although andesites can be produced by the melting of mantle material saturated with an aqueous fluid (Mysen and Boettcher, 1975; Hirose, 1997), the genesis of typical low-Mg andesitic magmas at island arcs is commonly referred to the processes of the

deep fractionation of parental mantle magmas under crustal conditions, with the participation of country-rock assimilation and mixing (Gill, 1981; Carmichael, 2002; Tolstykh *et al.*, 2003).

The knowledge of composition of parental arc magmas is of crucial importance for understanding the composition of the continental crust, which is generated within island arcs, and for evaluating the efficiency of the recycling of crustal material in subduction zones and the global compositional evolution of the Earth's mantle (see, for example, Hofmann, 1988). The complex character of the differentiation of arc magmas

makes it extremely difficult to evaluate the compositions of their parental melts. In spite of the significant number of publications devoted to the conditions of mantle melting in suprasubduction zones, this problem remains among the most disputable issues of petrology and geochemistry, mostly because of the paucity of reliable evaluations of the compositions of parental island-arc magmas. Because of this, every find of high-Mg island arc rocks is of significant petrological interest and provides a rare possibility of assaying the composition of the parental mantle melts and testing models for arc magmatism. At the same time, identification of high-Mg basalts with mantle melts is not always warrantable. These rocks are often of cumulative genesis, and their high Mg# is caused by their richness in mafic minerals but not by their poor differentiation (Sobolev *et al.*, 1993; Danyushevsky *et al.*, 2002). A source of the mafic minerals can also be mantle xenoliths disintegrated in the magma. These phenomena can significantly affect evaluations of the compositions of the parental melts, and this possibility should always be analyzed when the compositions of primitive arc basalts are interpreted.

Kamchatka is one of the world's most active volcanic areas. As in continental margins of the convergent type elsewhere, the volcanic products of Kamchatkan volcanoes are dominated by evolved rock varieties: andesites and basaltic andesites. High-Mg basalts are present in strongly subordinate amounts, and occur as significant volumes of lavas only in the Northern Group of volcanoes (*Active Volcanoes…*, 1991). In 1935 A.N. Zavaritskii described high-Mg megaphyric olivine–pyroxene rocks from Avachinsky volcano (Zavaritskii, 1935), which were unique in Kamchatka and later received the name of avachites (Kutyev *et al.*, 1980). The examination of these rocks was always accompanied by a discussion of their genesis, the localization and succession of the volcanic events, and relations with volcanics of other series (Shcheka *et al.*, 1978; Kutyev *et al.*, 1980; Ivanov and Plyusnin, 1988). Interest in avachites was revived after the discovery of fine-grained diamond aggregates (carbonado) in them (Baikov *et al.*, 1995; Gorshkov *et al.*, 1995), which gave rise to alternative models for the genesis of these rocks.

This paper generalizes preexisting data on the major- and trace-element geochemistry of avachites and presents the results of a systematic examination of their mineralogy, evaluations of the composition of their parental melts, and the conditions under which these melts were derived and crystallized, as can be inferred from the chemistry of the rocks and their minerals. Data on melt inclusions in olivine phenocrysts from these rocks will be reported in the second part of this publication (Portnyagin *et al.*, 2005).

## GENERAL CHARACTERISTICS OF AVACHITES

Volcanism in Kamchatka is induced by the subduction of the Pacific plate beneath the Eurasian continental margin. Active Kamchatkan volcanoes are concentrated within its Eastern Volcanic Belt, which consists of a southern, eastern, and a northern segment (*Active volcanoes…*, 1991; Fig. 1). Avachinsky is the southernmost volcano in the volcanic front of the Eastern Segment. Together with rear Koryakskii volcano and the extinct volcanoes of Kozel'skii, Aag, and Arik, Avachinsky forms one of the largest volcanic centers in Kamchatka.

Avachites were found as rounded fragments and boulders up to 5 m across in the streambed of the Mutnaya River in the northeastern part of the Avachinsky volcanic edifice. These fragments were traced throughout the whole course of the Mutnaya River up to its source at the Zavaritskii Glacier. Neither the setting of avachites in the volcanic edifice nor their affiliation to some volcanic facies were determined reliably, and there seems to be no primary exposures of these rocks. The onset of the denudation of the source of these rocks was dated based on the occurrence of avachite boulders in the deposits of a glaciofluvial terrace in the walls of the Mutnaya River valley, which seems to have provided these rocks for the riverbed alluvium. These glaciofluvial deposits are "imbedded" in a moraine of the latest glacial period and were dated at the end of Late Pleistocene based on tephrochronological evidence (L.I. Bazanova, personal communication). The primary source of avachites is believed to have been one of the lava bodies of the ancient Avachinsky edifice, which was produced in the Middle Pleistocene (*Active volcanoes…*, 1991).

Avachites are massive rocks of gray color, with large phenocrysts (Fig. 2a), whose amount varies from 35 to 55% and the sizes reach 15–20 mm. The phenocryst minerals are olive green or, sometimes, reddish limonitized olivine and bottle green to brown clinopyroxene. Phenocrysts of plagioclase, orthopyroxene, and spinel are rare (Table 1). The identified accessory minerals are magnetite, ilmenite, zircon, osmian iridium, rutile, and apatite (Kutyev *et al.*, 1980). Baikov *et al.* (1995) and Gorshkov *et al.* (1995) described carbonado, which was extracted from a 150-kg avachite sample. Xenoliths in avachites consist of spinel peridotites, olivinites, gabbro, and norites and are as large as 10 cm (Kutyev *et al.*, 1980).

Avachites have a composition corresponding to basalts and picrites of normal alkalinity (49.4–52.6 wt % $SiO_2$, 1.3–2.3 wt % $Na_2O + K_2O$, 14.1–19.7 wt % MgO). In the geochemical systematics of Kamchatkan volcanic rocks, avachites principally differ from other volcanics in having high Mg# and being unusually strongly enriched in refractory trace elements (Ni, Cr, and Os; Table 1, Fig. 3). In our database of analyses of volcanic rocks from Kamchatka (1650 analyses, available on request from the authors), only seven samples of rocks other than avachites have Mg# [here and below Mg# = 100Mg/(Mg + Fe), mol %] greater than 73, and, hence, can be regarded as undifferentiated mantle melts
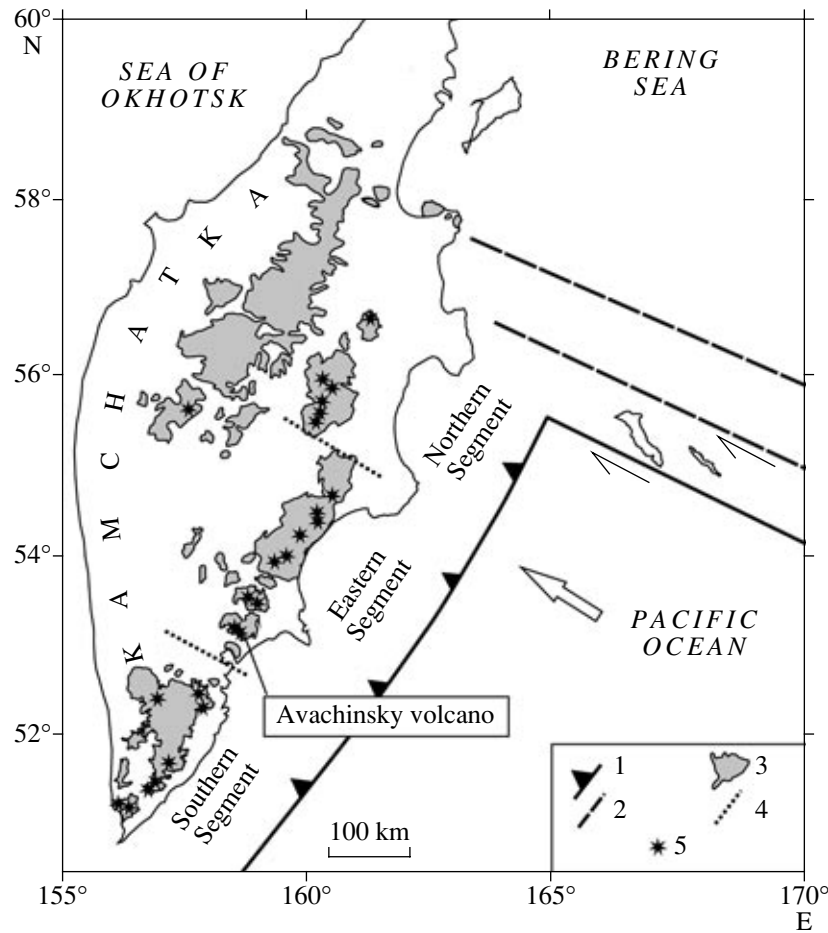
**Fig. 1.** Schematic map of the Quaternary volcanic belts of Kamchatka.
(1) Trench; (2) system of transform faults of the western termination of the Aleutian island arc; (3) Quaternary volcanic rocks in Kamchatka; (4) boundaries between the volcanic zones of Kamchatka; (5) active volcanoes, data from (*Active volcanoes…*, 1991).

that were in equilibrium with olivine more magnesian than $Fo_{90}$ (see, for example, Jaques and Green, 1980) (Fig. 3a). All of these primitive basalts and andesites were found in the Northern Group of volcanoes (Sheveluch, Zarechnyi, and Kharchinskii) (Volynets *et al.*, 2000). Avachites are more magnesian than any rock found elsewhere in Kamchatka. Their $TiO_2$, $Al_2O_3$, and $Na_2O$ contents are somewhat lower than the ranges typical of Kamchatkan basalts, but the abundances of other elements fall within these ranges.

The concentrations of incompatible trace elements of avachites are 1.5–2 times lower than in common basalts from Kamchatka (Fig. 4). The shape of the normalized trace element patterns is typical of arc lavas. Similarly to most Kamchatkan basalts, avachites are weakly enriched in LREE and strongly in Rb, K, Ba, and Sr at a Nb deficit relative to La and K, which testifies to similar processes of their generation. The $^{18}O/^{16}O$ isotopic ratio of avachites is slightly higher than the values typical of the mantle and mid-oceanic ridge basalts (MORB) but are quite typical of basalts in Kamchatka (Volynets, 1994; Pineau *et al.*, 1999; Bin-

deman *et al.*, 2004). The Sr, Nd, Pb, and Os isotopic ratios of avachites vary within the ranges of Kamchatkan Quaternary lavas and characterize the source mantle as analogous to the MORB source (Nd and Os isotopes) modified by the introduction of a component enriched in radiogenic Sr and Pb. The probable source of this component (possibly, a fluid) could be hydrothermally altered basalts in the subducted plate with an admixture of sedimentary material (see, for example, Kepenzhinskas *et al.*, 1997).

The geochemistry of avachites was characterized fairly thoroughly by earlier researchers. This paper is centered on the mineralogy of these rocks and the evaluation of the physicochemical parameters under which this unusual mineral assemblage was produced.

### METHODS

Minerals were analyzed in polished rock sections and in individual grains imbedded in epoxy pellets and polished with diamond pastes and corundum. The chemistry of minerals was determined by X-ray micro-
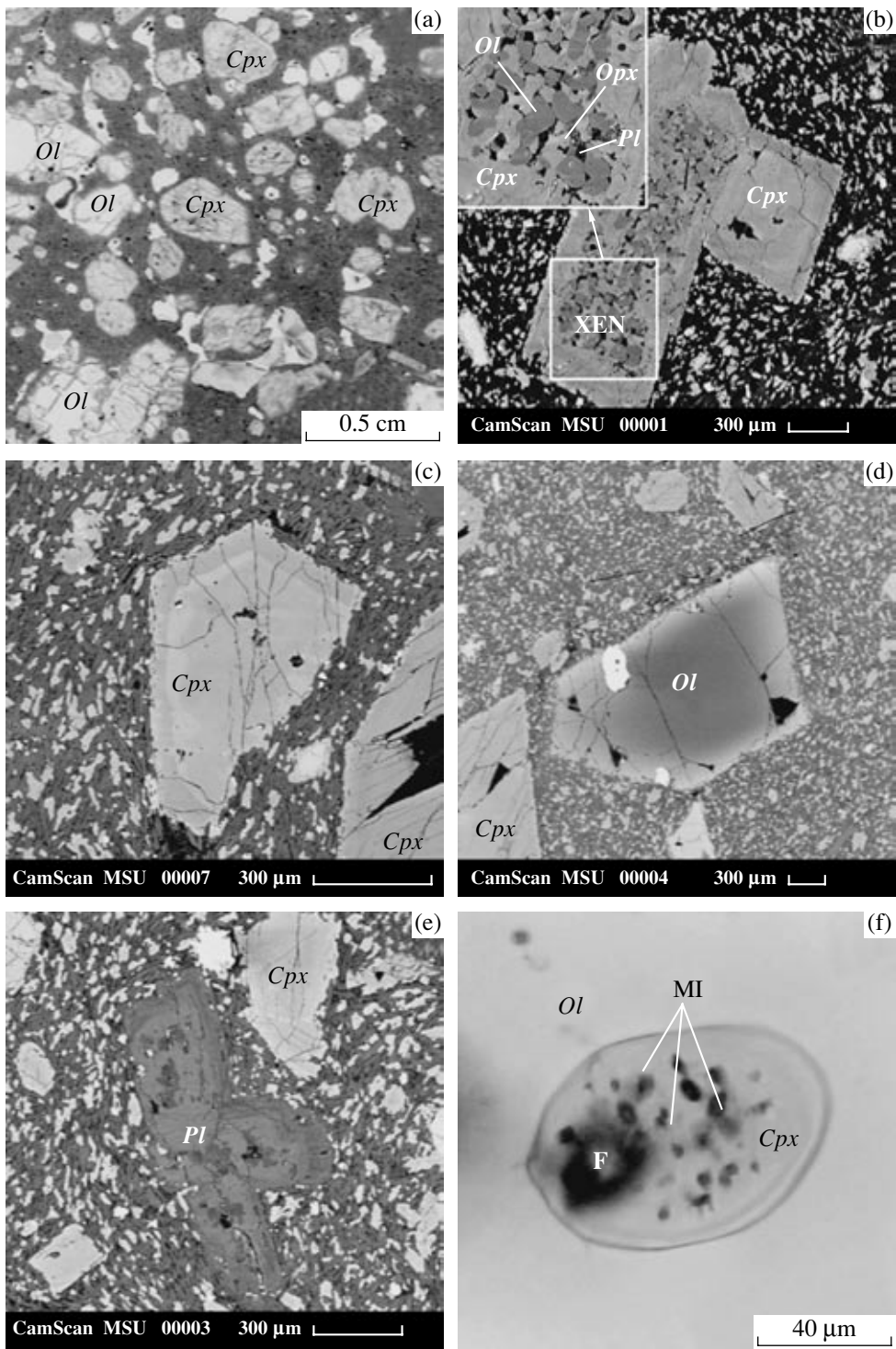
**Fig. 2.** Petrographic features of avachites.

(a) Transmitted-light microphotograph of avachite in a thin section, showing the texture and structure of the rocks determined by large olivine (*Ol*) and clinopyroxene (*Cpx*) crystals in a fine-grained groundmass.

(b) Large clinopyroxene crystal with included troctolite xenoliths (*Ol + Opx + Pl*). An enlarged fragment of this xenolith is shown in the inset. BSE image.

(c) Fragment of a clinopyroxene crystal with a weakly zoned ferrous core and a more magnesian outer part. The groundmass of the rock, consisting of magnetite (white), clinopyroxene (pale gray), plagioclase (dark gray), and glass (black), has a clearly pronounced trachytic texture, which is typical of volcanic rocks. BSE image.

(d) Euhedral olivine crystal of the second population with normal zoning. BSE image.

(e) Aggregate of plagioclase crystals with complicated mosaic (in the core) and cyclic (in the periphery) zoning. BSE image.

(f) Clinopyroxene inclusion in olivine. The pyroxene grain was captured together with a fluid bubble (F). The pyroxene contains numerous tiny melt inclusions (MI). Micrograph in transmitted light.

probe analysis on Camebax-microbeam and Cameca SX-50 microprobes (at the Vernadsky Institute and IfM-GEOMAR, respectively) with WDS and on a CamScan-4DV electron microscope equipped with a Link-10 000 EDS analytical setup (at the Moscow State University). Microprobe analyses were conducted at an accelerating voltage of 15 kV and a current of 10 nA for glasses and 50 nA for minerals. Analyses on the Cam-Scan electron microscope were performed at 15 kV accelerating voltage and 10 nA current. The typical analytical errors were 1–5% for major elements and 5−15% for trace elements at their concentrations of <1 wt %. The analytical calibration was conducted on natural standards of olivine (USNM 11312/444), augite (USNM 12214), chromite (USNM 117075), plagio-clase (USNM 115900), and ilmenite (USNM 96189) (Jarosewich *et al.*, 1980).

Trace-element concentrations in clinopyroxene were determined by second-ion mass spectrometry (SIMS) on a Cameca ims-4f ion microprobe at the Insti-
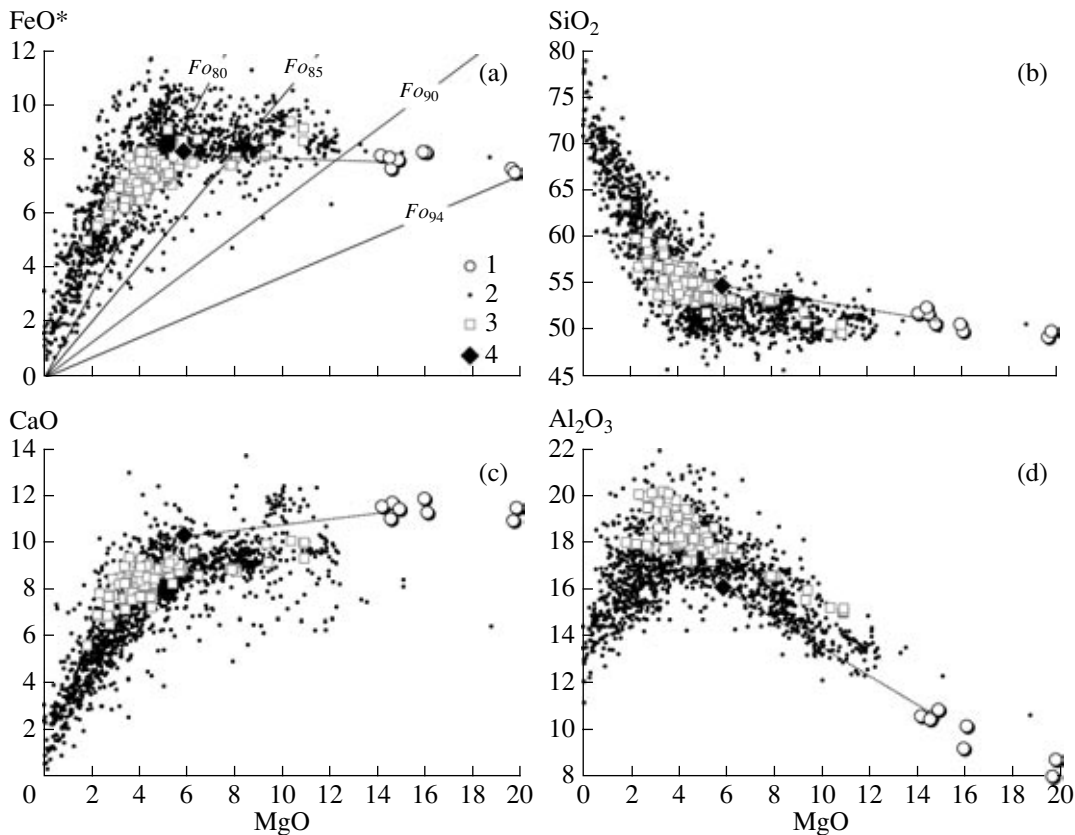


**Fig. 3.** Concentrations (wt %) of major elements in avachites.

(1) Avachite (see Table 1 for the data sources); (2) Quaternary volcanic rocks of Kamchatka (numerous sources); (3) rocks of Avachinsky volcano (Castellana, 1998); (4) calculated composition of the avachite groundmass (see text and Table 10).

In (a), solid lines indicate the composition of melts in equilibrium with olivine of different composition, calculated by the model (Ford *et al.*, 1983) at an oxygen fugacity corresponding to the Ni–NiO buffer.

**Table 1.** Chemical and modal compositions of avachites

| Major elements, wt %[1] | | Modal composition, vol %[3] | |
|---|---|---|---|
| SiO$_2$ | 49.40–52.56 (50.89) | Olivine | 13 (22–29) |
| TiO$_2$ | 0.20–0.71 (0.52) | | |
| Al$_2$O$_3$ | 8.00–10.84 (9.68) | Clinopyroxene | 24 (17–33) |
| Fe$_2$O$_3$ | 0.99–3.21 (2.21) | | |
| FeO | 5.46–6.71 (6.15) | Plagioclase | <1 (1) |
| MnO | 0.13–0.25 (0.16) | | |
| MgO | 14.11–19.74 (16.10) | Orthopyroxene | <1 (–) |
| CaO | 11.00–11.94 (11.56) | | |
| Na$_2$O | 0.76–1.92 (1.57) | Spinel | <2 (4–5) |
| K$_2$O | 0.26–0.54 (0.36) | | |
| P$_2$O$_5$ | 0.06–0.15 (0.09) | Groundmass | 60 (45–65) |
| H$_2$O | 0.75 | | |
| Total | 97.78–99.40 (99.11) | | |
| Trace elements, ppm[2] | | Isotopic ratios[4] | |
| Cs | 0.21 | $\delta^{18}O$ | 6.49 |
| Rb | 4 | | |
| Sr | 124–220 | $^{87}Sr/^{86}Sr$ | 0.70335 |
| Ba | 132–227 | | |
| La | 2.93 | $^{143}Nd/^{144}Nd$ | 0.51307 |
| Ce | 6.9 | | |
| Nd | 4.8 | $^{206}Pb/^{204}Pb$ | 18.427 |
| Sm | 1.6 | | |
| Eu | 0.54 | $^{207}Pb/^{204}Pb$ | 15.526 |
| Tb | 0.31 | | |
| Yb | 1.1 | $^{208}Pb/^{204}Pb$ | 38.155 |
| Lu | 0.157 | | |
| Y | 8.7–14 | $^{187}Os/^{188}Os$[5] | 0.133 |
| Zr | 23–47 | | |
| Nb | 0.5 | | |
| Hf | 1.03 | | |
| Th | 0.45 | | |
| Sc | 41.5–44.3 | | |
| V | 171–200 | | |
| Cr | 1023–1460 | | |
| Co | 48.3 | | |
| Ni | 330–380 | | |
| Os (ppt)[5] | 46 | | |

Note: [1] Major-element concentrations are given after (Volynets, 1994; Kepezhinskas *et al.*, 1997; Bindeman *et al.*, 2004; Koloskov *et al.*, 2001; Kutyev *et al.*, 1980; Gorshkov *et al.*, 1995). Average values are given in parentheses.

[2] Trace-element concentrations (except Os) are given after (Volynets, 1994; Kepezhinskas *et al.*, 1997).

[3] The modal composition of typical avachite is given according to the authors' data (counting of 8932 spots in a thin section) and, in parentheses, after (Kutyev *et al.*, 1980).

[4] The O, Sr, Nd, and Pb isotopic composition was borrowed from (Bindeman *et al.*, 2004).

[5] The Os isotopic composition and concentration was compiled from (Alves *et al.*, 2002).
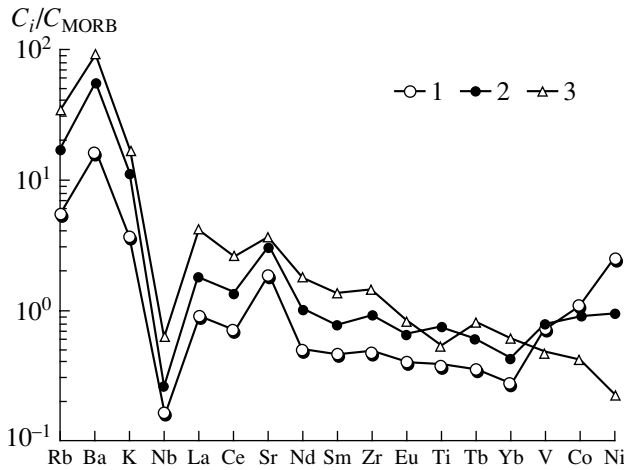
**Fig. 4.** N-MORB (Hofmann, 1988) normalized trace-element concentrations in avachites.

(1) Avachite (see Table 1 for the data sources); (2) average composition of calc–alkaline magnesian basalts in Kamchatka (Popolitov and Volynets, 1981); (3) average composition of calc–alkaline andesites in Kamchatka (Popolitov and Volynets, 1981).
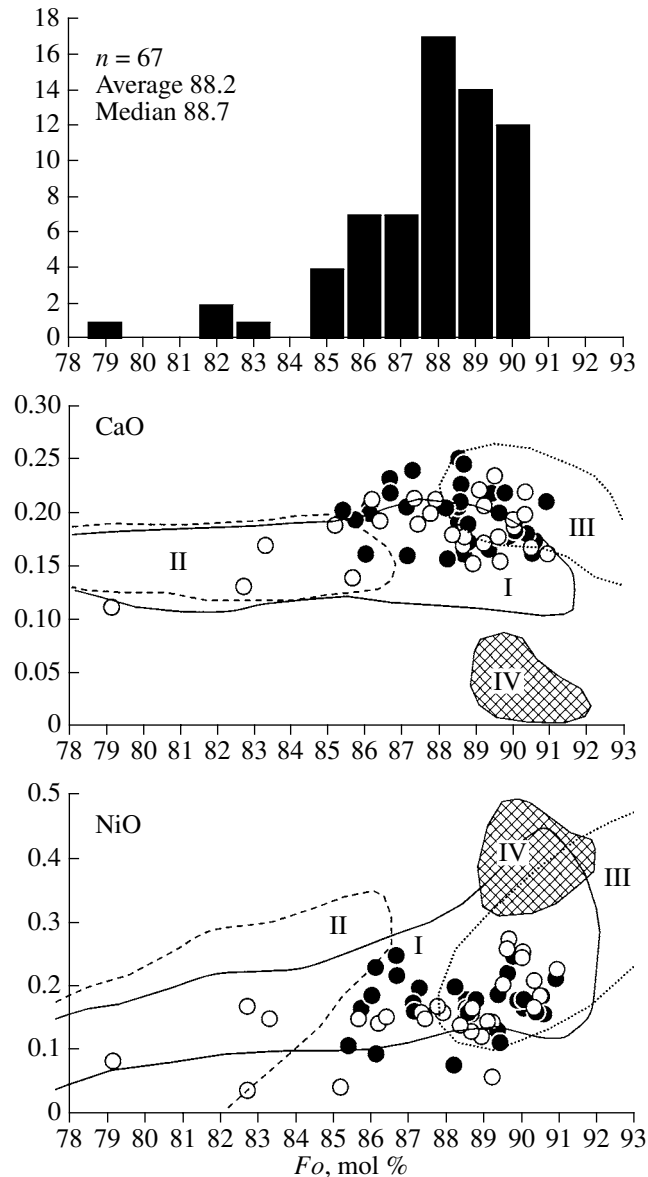


**Fig. 5.** Composition of olivine phenocrysts in avachites. Open circles—olivine without clinopyroxene inclusions, solid circles—olivine with clinopyroxene inclusions. Fields: I—olivine from Klyuchevskoy volcano (Kersting and Arculus, 1994; Ozerov, 2000; Mironov et al., 2001; our unpublished data), II—olivine from lavas in southern Kamchatka (M. Portnyagin, unpublished data), III—olivine in high-Ca boninites of Cyprus (Sobolev et al., 1993; Portnyagin et al., 1996), IV—olivine in disintegrated xenoliths in lavas of eastern Kamchatka (M. Portnyagin, unpublished data). Oxide concentrations are given in wt %.

tute of Microelectronics, Russian Academy of Sciences, Yaroslavl, accurate to 10–15% at concentrations of more than 1 ppm and 15–30% at concentrations of 0.1–1 ppm. The detection limits for different elements were within the range of 0.01–0.001 ppm. The standards were NIST-610 (Rocholl et al., 1997) and KL-2G (Jochum et al., 2000) and were analyzed in the same series as the samples.

The IR absorption spectra of $OH^-$ groups in olivine were examined on a Nicole 800 spectrometer with a microscope at the Department of Geology of the Bristol University, Great Britain. The IR spectra were collected at room temperature within the range of frequencies of 600 to 6000 $cm^{-1}$ with a spectral resolution of 4 $cm^{-1}$. The measurements were conducted in doubly polished platelets ~300 μm thick, which were prepared of individual olivine grains. The analytical spots were from 75 to 100 μm in diameter. The method is described in detail in (Matveev et al., 2005).

## MINERALOGY

### *Olivine*

Olivine phenocrysts in avachites compose two populations. Olivine of the first of them occurs as large anhedral grains from 1.5 mm to 2 cm across, which are partly corroded and are sometimes fragments of larger grains. Their cores are unzoned and vary in composition from $Fo_{85}$ to $Fo_{91}$, with the predominance of magnesian varieties ($Fo_{88–90}$; Fig. 5, Tables 2 and 3). The outermost rims consist of more ferrous olivine with zoning to $Fo_{79–83}$. Olivine grains of the second population are smaller (0.5–1 mm), euhedral, and have normal zoning (Fig. 2d). This olivine is high in Ca

(0.15–0.25 wt % CaO) and is mildly enriched in Ni (0.25–0.05 wt % NiO). The CaO and NiO concentrations do not correlate with the Mg# of this mineral. Olivine in avachites is much more magnesian than this mineral in lavas in the Southern Segment of the Kamchatka arc and is close in composition to olivine from the Central Kamchatkan Depression, including olivine

**Table 2.** Composition (wt %) of coexisting olivine and clinopyroxene

| Component | 3/1* | cpx4 | 3/2 | cpx2 | cpx6b | cpx6a | cpx3 | av4f | cpx1 | 2ol2 | 2ol1 |
|---|---|---|---|---|---|---|---|---|---|---|---|
| | *Ol*** | *Cpx* | *Ol* | *Cpx* | *Cpx* | *Cpx* | *Cpx* | *Ol* | *Cpx* | *Cpx* | *Cpx* |
| | *Cpx**** | *Ol* | *Cpx* | *Ol* | *Ol* | *Ol* | *Ol* | *Cpx* | *Ol* | *Ol* | *Ol* |
| Clinopyroxene | | | | | | | | | | | |
| $SiO_2$ | 54.59 | 53.23 | 54.57 | 53.45 | 53.43 | 53.78 | 53.62 | 54.46 | 53.00 | 50.99 | 50.44 |
| $TiO_2$ | 0.10 | 0.11 | 0.22 | 0.11 | 0.16 | 0.21 | 0.16 | 0.17 | 0.23 | 0.47 | 0.45 |
| $Al_2O_3$ | 1.08 | 1.23 | 1.73 | 1.13 | 1.35 | 1.51 | 1.35 | 1.41 | 2.32 | 3.02 | 2.89 |
| FeO | 2.69 | 2.82 | 2.99 | 2.97 | 3.23 | 3.2 | 3.36 | 3.66 | 4.26 | 6.51 | 6.98 |
| MnO | 0.07 | 0.11 | 0.05 | 0.07 | 0.1 | 0.11 | 0.14 | 0.12 | 0.14 | 0.21 | 0.17 |
| MgO | 18.09 | 18.28 | 18.00 | 18.08 | 17.85 | 17.56 | 17.82 | 17.46 | 16.55 | 16.12 | 16.08 |
| CaO | 22.38 | 22.79 | 22.81 | 22.65 | 23.05 | 22.8 | 22.75 | 22.57 | 22.48 | 21.73 | 21.33 |
| $Na_2O$ | 0.24 | 0.19 | 0.24 | 0.23 | 0.19 | 0.22 | 0.27 | 0.19 | 0.26 | 0.21 | 0.25 |
| $Cr_2O_3$ | 0.74 | 0.71 | 1.06 | 0.45 | 0.53 | 0.37 | 0.49 | 0.47 | 0.27 | 0.02 | 0.01 |
| Total | 99.98 | 99.47 | 101.67 | 99.14 | 99.89 | 99.76 | 99.96 | 100.51 | 99.51 | 99.29 | 98.59 |
| Mg#, mol % | 92.3 | 92.0 | 91.5 | 91.6 | 90.8 | 90.7 | 90.4 | 89.5 | 87.4 | 81.5 | 80.4 |
| Olivine | | | | | | | | | | | |
| $SiO_2$ | 40.07 | 40.70 | 40.07 | 39.67 | 39.91 | 39.74 | 39.63 | 40.68 | 38.85 | 39.00 | 39.61 |
| FeO | 11.36 | 9.37 | 11.36 | 11.68 | 10.88 | 13.67 | 11.92 | 11.00 | 15.75 | 19.57 | 16.43 |
| MnO | 0.12 | 0.15 | 0.12 | 0.25 | 0.2 | 0.22 | 0.15 | 0.15 | 0.25 | 0.34 | 0.31 |
| MgO | 48.45 | 49.15 | 48.45 | 47.05 | 47.75 | 45.86 | 46.55 | 48.42 | 44.1 | 41.68 | 44.12 |
| CaO | 0.18 | 0.22 | 0.18 | 0.20 | 0.17 | 0.14 | 0.19 | 0.18 | 0.17 | 0.11 | 0.13 |
| NiO | 0.14 | 0.21 | 0.14 | 0.17 | 0.13 | 0.15 | 0.15 | 0.17 | 0.15 | 0.08 | 0.04 |
| $Cr_2O_3$ | | 0.04 | | 0.07 | 0.00 | 0.00 | 0.02 | | 0.06 | 0.00 | 0.00 |
| Total | 100.32 | 99.84 | 100.32 | 99.09 | 99.04 | 99.78 | 98.61 | 100.60 | 99.33 | 100.79 | 100.64 |
| *Fo*, mol % | 88.4 | 90.3 | 88.4 | 87.8 | 88.7 | 85.7 | 87.4 | 88.7 | 83.3 | 79.2 | 82.7 |

Note: * Sample; ** host mineral; *** inclusion. Analyses were conducted at the Vernadsky Institute of Geochemistry and Analytical Chemistry (GEOKhI), Russian Academy of Sciences.

from Klyuchevskoy volcano (Khubunaya *et al.*, 1993; Kersting and Arculus, 1994; Ariskin *et al.*, 1995) (Fig. 5) but differs from the latter in having somewhat higher Ca contents and no Ni-rich compositions. A close analogue of olivine from avachites is moderately magnesian olivine in high-Ca boninites (Sobolev and Danyushevsky, 1994; Sobolev *et al.*, 1993; Portnyagin *et al.*, 1996). Its high Ca concentration makes the olivine in avachites principally different from this mineral in disintegrated mantle xenoliths in Kamchatkan lavas (Fig. 5).

IR spectroscopic data demonstrate that the OH⁻ group is incorporated into the structures of most of the olivine crystals, as follows from the intense absorption bands within the frequency range of 3100–3700 cm⁻¹ (Fig. 6). The calculated $H_2O$ concentrations in olivine from avachites is 0.5 ± 0.1 ppm. The $H_2O$ concentration in the equilibrium melt, which was calculated using the $H_2O$ distribution coefficients at pressures of about 300 MPa (Hirth and Kohlstedt, 1996) is 0.5 ± 0.1 wt %.

These estimates should be regarded as the lower limit, because olivine can easily loose $H_2O$ if the physico-chemical conditions change during magma crystallization and eruption (Matveev *et al.*, 2005).

Similar and higher values of $H_2O$ concentration in olivine were also found in other arc magmas, including boninites (Matveev *et al.*, 2005). In contrast to avachites, olivine in high-Ca boninites shows an $H_2O$ absorption band in another region of the IR spectrum (3380–3285 cm⁻¹). As was discussed in detail in (Matveev *et al.*, 2001, 2005), the position of the absorption bands caused by the OH⁻ group is determined by its structural setting (in the tetrahedral or the octahedral site) in olivine. The occurrence of different structural vacancies that can be occupied by the OH⁻ group is, in turn, dependent on the silica activity in the crystallizing magma. Olivine crystallizing from magmas saturated with $SiO_2$ and with orthopyroxene as a liquidus phase (for instance, boninites) contains the OH⁻ group in the octahedral site. Olivine in avachites contains the OH⁻

group in the tetrahedral site and, hence, could crystallize from melts with low $SiO_2$ activities and strongly undersaturated in orthopyroxene. This conclusion is in conflict with the hypersthene-normative bulk composition of avachites and the occurrence of ferrous orthopyroxene in these rocks but is, in our opinion, of significant petrological importance, as will be discussed below.

### Clinopyroxene

Clinopyroxene develops as large (from 1–2 mm to 2 cm) crystals or often occurs as their fragments or as rims overgrowing small xenoliths of olivine gabbro and norites (Figs. 2b, 2c). Many crystals of this mineral have weakly zoned round cores with traces of resorption. The outer zones of the crystals exhibit complicated cyclic, often reverse, zoning, which is clearly seen in BSE images (Fig. 2c). The composition of clinopyroxene broadly varies (Mg# = 92.5–72.5 mol %, Fig. 7, Table 2) with the predominance of magnesian varieties, which commonly compose crystal cores. As the Mg# of the mineral decreases, the pyroxene depletes in $SiO_2$, CaO, and $Cr_2O_3$ but enriches in $TiO_2$, $Al_2O_3$, and $Na_2O$, as is characteristic of the compositional evolution of this mineral during the crystallization of primitive basaltic magmas. The presence of magnesian pyroxene is atypical of lavas in southern Kamchatka (Popolitov and Volynets, 1981; our unpublished data). Analogous to olivine, clinopyroxene of similar composition was found only in lavas in the Central Kamchatkan Depression. Compared to Klyuchevskoy volcano, many pyroxenes from avachites are more magnesian, less aluminous (Mg# = 91.0–92.5 mol %, $Al_2O_3$ = 0.95–1.20 wt %), and have relatively low concentrations of $SiO_2$, $Na_2O$, and $Cr_2O_3$ and high CaO contents. The extremely high Mg# of these pyroxenes makes avachites similar to high-Ca boninites (Sobolev et al., 1993), but, unlike pyroxenes in boninites, this mineral in avachites exhibits elevated concentrations of CaO and $Na_2O$ at low $SiO_2$ (Fig. 7). These features of pyroxene in avachites are explained by the elevated fractions of the diopside and hedenbergite components and the relatively low fractions of the enstatite and ferrosilite components in this mineral as compared with pyroxene in rock of Klyuchevskoy volcano and boninites. The contents of the jadeite component in the pyroxene from avachites are intermediate between those in pyroxenes from the rock groups mentioned above. Compared to pyroxenes in the mantle xenoliths of Avachinsky volcano, pyroxene in avachites is less magnesian, lower in $Al_2O_3$, and higher in $TiO_2$ (Fig. 7).

Concentrations of trace elements were analyzed in a magnesian phenocryst (Mg# = 92.3 mol %) and in a pyroxene inclusion (Mg# = 92.0 mol %) in olivine $Fo_{88.4}$ (Fig. 8, Table 4). Both of the analyzed pyroxenes were practically identical in composition and were characterized by weak enrichment in MREE relative to HREE $[Sm/Yb]_N$ = 1.6–2.1 and depletion in LREE $[La/Sm]_N$ = 0.17–0.22. The normalized concentrations
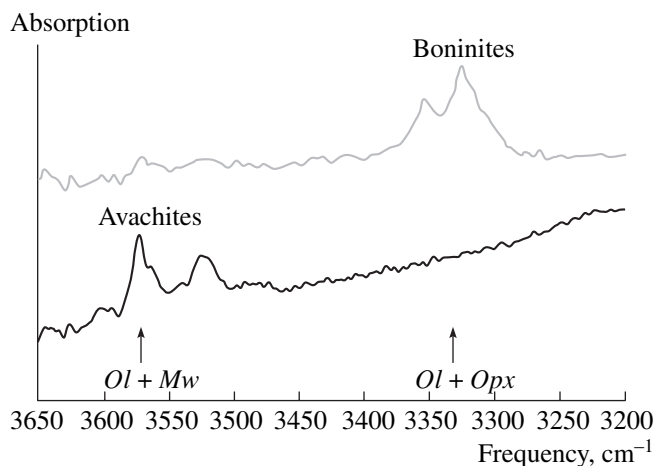


**Fig. 6.** IR absorption spectra of olivine from avachites in comparison with the spectra of olivine from high-Ca boninites (Matveev et al., 2005).

Arrows indicate the approximate position of the absorption bands of the $OH^-$ group in olivine synthesized in equilibrium with orthopyroxene (Ol + Opx, high $aSiO_2$) and in equilibrium with Mg-wuestite (Ol + Mw, low $aSiO_2$) (Matveev et al., 2001).

of Zr, Ba, and K are ten to twenty times lower than those of LREE. Conversely, the Sr concentration is fourfold that of Ce. The Th, Be, and B concentrations are of the same order as the LREE contents. The contents of Zr and HREE in pyroxene from avachites are close to the contents of these elements in the pyroxene of high-Ca boninites from Cyprus (Sobolev et al., 1996), while the concentrations of Sr, LREE, and MREE in the pyroxene are close to those in the most magnesian pyroxenes in basalts of the Aleutian island arc (Yogodzinsky and Kelemen, 1998). Pyroxenes in magnesian andesites from the Commander Islands and Adak Island differ from pyroxene in avachites in having much higher concentrations of all incompatible elements (Yogodzinsky and Kelemen, 1998).

The simultaneous occurrence of high-Mg pyroxene and olivine in the early liquidus assemblage of avachites is also reflected in the presence of mutual inclusions of these minerals in one another (Fig. 2f). Nearly 50% of the olivine crystals examined in the course of our research contained pyroxene inclusions (Fig. 5), and olivine inclusions in pyroxene are also quite usual. The compositions of the inclusions and their host minerals are clearly correlated (Fig. 9), a fact testifying that the minerals crystallized simultaneously starting in the earliest evolutionary stages of the parental melt. Analogous relations between olivine and pyroxene are also typical of the lavas of Klyuchevskoy volcano (Khubunaya et al., 1993; Ariskin et al., 1995; Ozerov, 2000). The composition of the crystalline inclusions does not differ from those of the corresponding phenocryst minerals, including the trace-element compositions of pyroxene of different morphological types (Table 4, Fig. 8).
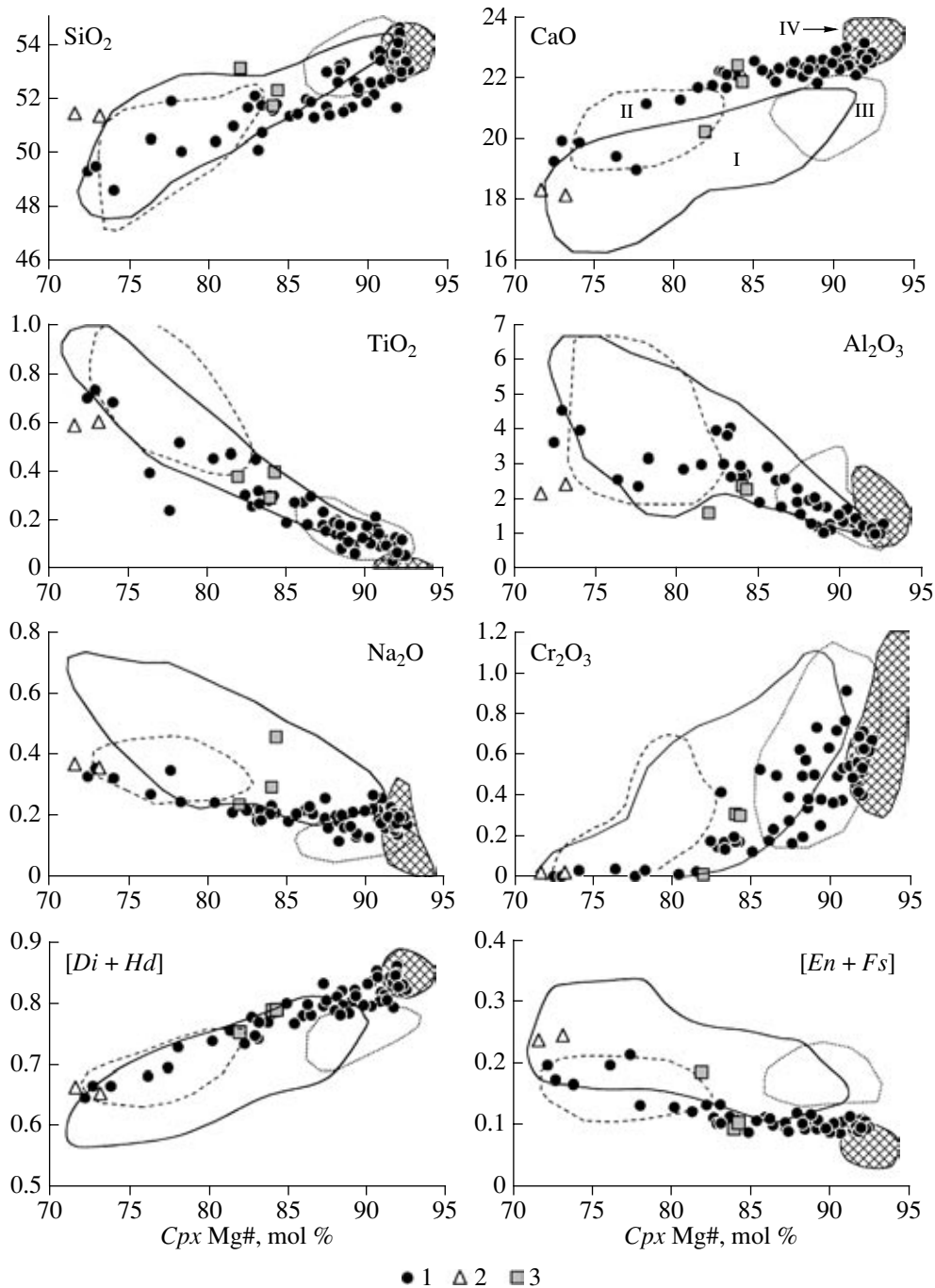
**Fig. 7.** Composition of clinopyroxene in avachites.

(1) Phenocrysts; (2) groundmass pyroxene; (3) pyroxene from xenoliths of intrusive rocks. Fields: I—clinopyroxene from Klyuchevskoy volcano (Kersting and Arculus, 1994; Ozerov, 2000; Mironov *et al.*, 2001; our unpublished data), II—clinopyroxene from lavas in southern Kamchatka (M. Portnyagin, unpublished data), III—clinopyroxene in high-Ca boninites of Cyprus (Sobolev *et al.*, 1993; Portnyagin *et al.*, 1996), IV—clinopyroxene in harzburgite xenoliths in lavas of Avachinsky volcano (Koloskov *et al.*, 2001). Oxide concentrations are given in wt %. Clinopyroxene components: *Di*—diopside, *Hd*—hedenbergite, *En*—enstatite, *Fs*—ferrosilite. Contents of components are given as mole fractions.

### *Spinel*

Cr-spinel occurs mostly as crystalline inclusions in olivine or, more rarely, as individual phenocrysts or inclusions in pyroxene. Most of the Cr-spinels are highly magnesian (Mg# = 51–61 mol %) and chromian

[Cr# = Cr/(Cr + Al) = 0.73–0.81) but are poor in $TiO_2$ (0.28–0.45 wt %) (Table 3, Fig. 10), having compositions intermediate between those of spinel from moderate- and high-K arc basalts, on the one hand, and low-K arc tholeiites and boninites, on the other
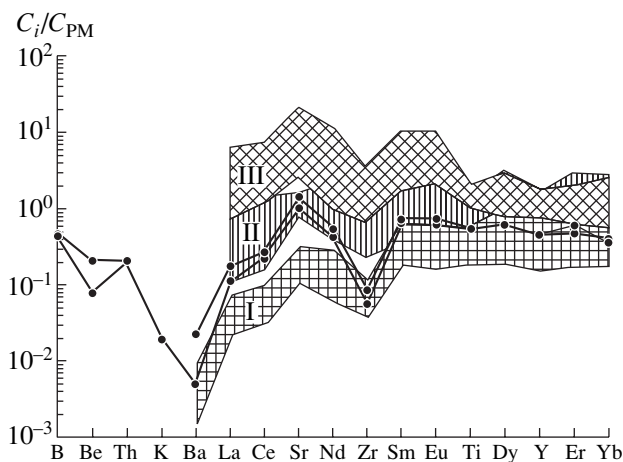
**Fig. 8.** Concentrations of trace elements in clinopyroxene from avachites.

Fields: I—clinopyroxene from high-Ca boninites in Cyprus (Sobolev *et al.*, 1996); II—high-Mg (Mg# > 88 mol %) clinopyroxene from basalt of the Aleutian arc (Yogodzinsky and Kelemen, 1998), III—clinopyroxene from adakites of the Aleutian arc (Yogodzinsky and Kelemen, 1998). Concentrations of elements are normalized to the primitive mantle (Sun and McDonough, 1989).

(Kamenetsky *et al.*, 2001). The spinel of avachites is close in composition to the most chromian and low-Ti spinel in the lavas of Klyuchevskoy volcano and significantly differs from the aluminous spinel in the typical lavas of southern Kamchatka (Fig. 10). Spinel in avachites differs from this mineral in mantle xenoliths from Avachinsky volcano (Koloskov *et al.*, 2001) in having a high Cr# and being more oxidized and Ti-rich. Some of the analyzed spinels included in high-Mg olivine are noted for elevated $TiO_2$ contents (1.4–5.0 wt %) and a high degree of Fe oxidation [$Fe^{3+}/(Fe^{3+} Al + Cr)$ = 0.15−0.6]. Conceivably, these spinel inclusions were captured by olivine late in the course of magma differentiation, when cracks in olivine were healed, and were not cotectic phases for the high-Mg host olivine.

### *Orthopyroxene*

Rare orthopyroxene crystals in avachites are low magnesian and low aluminous (Mg# = 74.3–65.3 mol %, 0.8–1.0 wt % $Al_2O_3$; Table 5). Orthopyroxene of similar composition is quite characteristic of basaltic andesites in Kamchatka (Volynets, 1994). More magnesian orthopyroxene was described as inclusions in olivine in the lavas of Klyuchevskoy volcano (Khubunaya *et al.*, 1993; Ozerov, 2000). No such crystalline inclusions were found in olivine from avachites. The absence of magnesian orthopyroxene from the phenocryst assemblage is an important petrogenetic feature that distinguished avachites from magmas of boninite type (Crawford *et al.*, 1989).
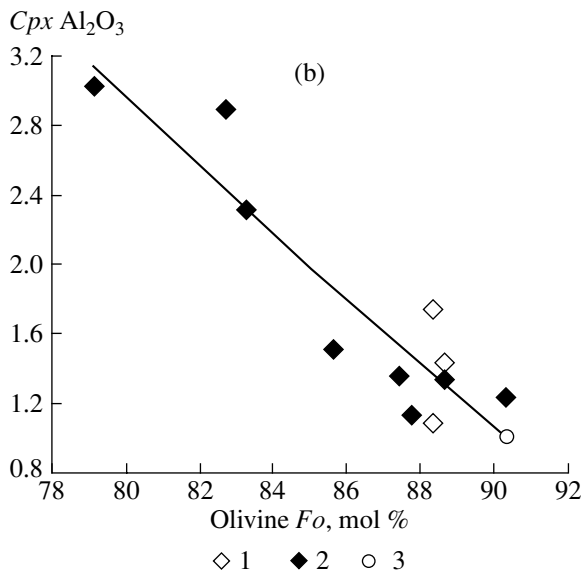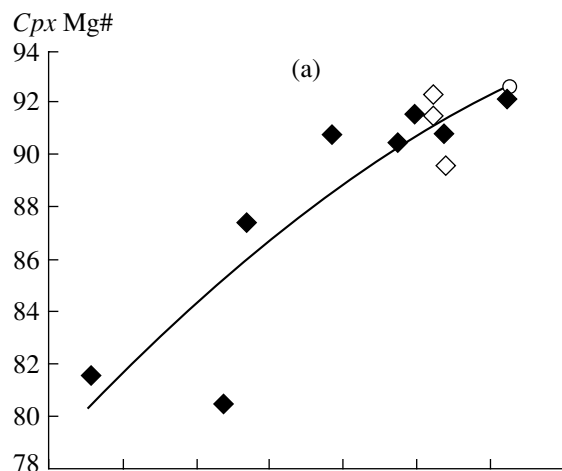
**Fig. 9.** Composition of coexisting olivine and clinopyroxene. (1) Pyroxene inclusions in olivine; (2) olivine inclusions in pyroxene; (3) composition of minerals of the liquidus assemblage (see text for explanations). $Al_2O_3$ concentrations are given in wt %, Mg# is in mol %.

### *Groundmass Minerals and Xenoliths*

The fine-grained groundmass of avachites has a trachytic texture (Fig. 2) and consists of plagioclase (~52 vol % $An_{68–73}$), clinopyroxene (~25 vol %, Mg# = 70–73 mol %), titanomagnetite (~5 vol %), ilmenite (<1 vol %), and silicic volcanic glass (~15 vol %) (Table 6). The high glass content in the groundmass testifies to rapid magma solidification upon eruption and, hence, the volcanic nature of avachites.

It was found out that avachites contain rare microxenoliths of olivine gabbro, troctolite, and strongly altered volcanic rocks with a hyalopilitic texture. These xenoliths occur as fragments in the groundmass of the rocks and are partly or completely embedded in clinopyroxene crystals or sometimes occur as inclusions in olivine (Fig. 2b, Table 7). Clinopyroxene
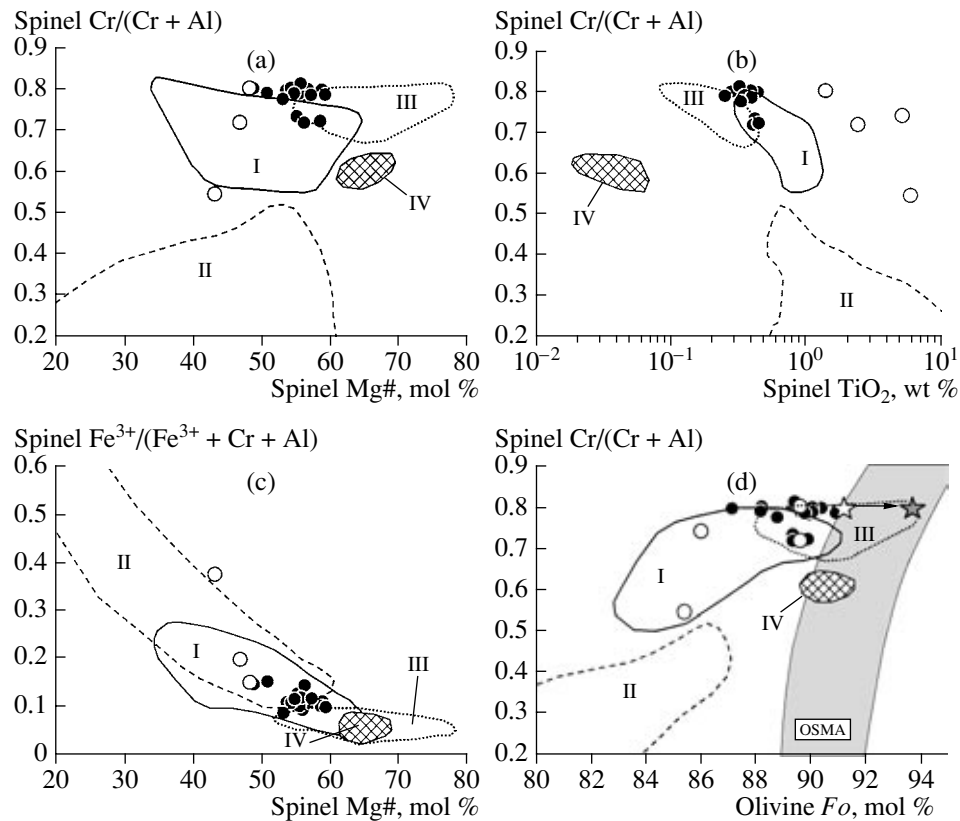
**Fig. 10.** Composition of Cr-spinel in avachites.

Solid circles—low-Ti spinel, open circles—high-Ti spinel. Fields: I—spinel from lavas of Klyuchevskoy volcano (Kersting and Arculus, 1994; Ozerov, 2000; Mironov *et al.*, 2001; our unpublished data), II—spinel from lavas in southern Kamchatka (M. Portnyagin, unpublished data), III—spinel in high-Ca boninites of Cyprus (Sobolev *et al.*, 1993; Portnyagin *et al.*, 1996), IV—spinel in harzburgite xenoliths in lavas of Avachinsky volcano (Koloskov *et al.*, 2001). The open star in Fig. 10d shows the composition of the most magnesian assemblage of olivine and spinel in avachites in equilibrium with melt AV-91 (Table 8); the gray star corresponds to the estimated composition of the liquidus assemblage of melt AV-94 (Table 8). *OSMA*—compositional field of the olivine–spinel assemblage in mantle rocks (Arai, 1994).

(Mg# = 76−82 mol %) from the xenoliths of intrusive rocks is compositionally close to phenocrysts in avachites (Fig. 7), and the orthopyroxene is somewhat more magnesian (Mg# = 76–84 mol %) than in the phenocrysts. Plagioclase ($An_{60-62}$) is notably more sodic than in the groundmass of avachites).

## DISCUSSION

### *Liquidus Assemblage of Avachites*

Our results demonstrate that, although avachites contain xenogenic material, the mineral assemblage of magnesian olivine, clinopyroxene, and spinel was not borrowed from disintegrated mantle xenoliths, which are abundant in the lavas of Avachinsky volcano (*Active volcanoes…*, 1991) but is of magmatic genesis. This follows from the differences between the compositions of the same minerals in avachites and mantle xenoliths (Figs. 5, 7, 10) and from the occurrence of primary melt inclusions in the olivine (Portnyagin *et al.*, 2005). The simultaneous occurrence of olivine, pyroxene, and spinel as rock-forming minerals and as mutual crystal-

line inclusions of these minerals in one another led us to conclude that the mineral assemblage is cogenetic and crystallized from the same cotectic melt.

Theoretically, the crystallization of the melt could be either fractional or equilibrium. In fractional crystallization, crystals are efficiently removed from the magmatic system and do not interact with the melt. In this situation, the most magnesian mineral assemblage in a rock can be regarded as the liquidus one. This assemblage in avachites consists of olivine ($Fo_{91}$), clinopyroxene (Mg# = 92.5 mol %), and Cr-spinel [Mg# ~ 60 mol %, Cr/(Cr + Al) ~ 0.8] (Table 8). Conversely, during equilibrium crystallization, the crystals continuously reequilibrate with the ambient melt under changing physicochemical conditions, and, hence, the compositions of the minerals composing the rock should significantly differ from those in the primary liquidus assemblage.

The possibility of perfect fractional or equilibrium crystallization is controlled by the relations between the rates of the removal of crystals from the system (for example, by means of their settling in the form of

**Table 3.** Representative compositions of inclusions of Cr-spinel in olivine and clinopyroxene phenocrysts

| Component | OL12* | OL2 | OL43a | OL36 core | OL36 margin | OL33 | OL25 | OL10 | OL37 | OL32 | OL20 | OL39 core | OL39 margin | CP10 |
|---|---|---|---|---|---|---|---|---|---|---|---|---|---|---|
| | Spl** | Spl | Spl | Spl core | Spl margin | Spl | Spl | Spl | Spl | Spl | Spl | Spl core | Spl margin | Spl |
| $SiO_2$ | 0.58 | 0.23 | 0.40 | 0.31 | 0.30 | 0.50 | 0.59 | 0.17 | 0.30 | 0.09 | 0.29 | 0.33 | 0.24 | 0.07 |
| $TiO_2$ | 0.34 | 0.44 | 0.28 | 0.36 | 0.45 | 0.39 | 0.35 | 0.32 | 0.36 | 0.39 | 5.02 | 1.38 | 2.38 | 0.43 |
| $Al_2O_3$ | 9.59 | 8.85 | 8.79 | 9.72 | 12.62 | 9.41 | 9.22 | 8.22 | 8.69 | 8.91 | 4.50 | 7.91 | 10.47 | 8.88 |
| $Cr_2O_3$ | 53.77 | 53.38 | 53.43 | 53.13 | 49.88 | 52.47 | 52.78 | 54.63 | 49.83 | 53.37 | 19.61 | 48.94 | 40.72 | 54.92 |
| $V_2O_3$ | 0.11 | 0.09 | 0.07 | 0.16 | 0.09 | 0.11 | 0.13 | 0.07 | 0.13 | 0.14 | 0.54 | 0.29 | 0.28 | |
| $FeO^{1)}$ | 15.31 | 15.07 | 15.80 | 16.10 | 15.46 | 15.96 | 16.95 | 16.22 | 17.83 | 16.79 | 31.49 | 19.11 | 20.19 | 14.48 |
| $Fe_2O_3^{2)}$ | 8.08 | 8.91 | 8.72 | 7.50 | 8.35 | 9.46 | 9.39 | 9.67 | 12.08 | 8.77 | 36.55 | 11.53 | 14.90 | 8.33 |
| $MnO$ | 0.27 | 0.24 | 0.27 | 0.25 | 0.31 | 0.27 | 0.27 | 0.31 | 0.25 | 0.20 | 0.39 | 0.29 | 0.28 | 0.00 |
| $MgO$ | 12.49 | 12.05 | 11.61 | 11.43 | 12.24 | 11.96 | 11.50 | 11.42 | 10.31 | 10.87 | 3.84 | 9.97 | 9.96 | 12.53 |
| $NiO$ | 0.03 | 0.10 | 0.11 | 0.09 | 0.22 | 0.11 | 0.07 | 0.13 | 0.10 | 0.09 | 0.07 | 0.12 | 0.07 | 0.09 |
| Total | 100.57 | 99.36 | 99.47 | 99.06 | 99.92 | 100.63 | 101.25 | 101.16 | 99.86 | 99.61 | 102.29 | 99.86 | 99.49 | 99.49 |
| $Mg/(Mg + Fe^{+2})$ | 0.592 | 0.588 | 0.567 | 0.559 | 0.585 | 0.572 | 0.547 | 0.557 | 0.507 | 0.536 | 0.179 | 0.482 | 0.468 | 0.607 |
| $Cr/(Cr + Al)$ | 0.790 | 0.802 | 0.803 | 0.786 | 0.726 | 0.789 | 0.793 | 0.817 | 0.794 | 0.801 | 0.745 | 0.806 | 0.723 | 0.806 |
| $Fe^{+2}/Fe^{+3}melt^{3)}$ | 7.5 | 6.4 | 7.0 | 8.8 | 7.2 | 6.4 | 7.0 | 6.3 | 5.4 | 7.6 | 2.7 | 6.3 | 4.8 | 6.7 |
| $\Delta QFM^{4)}$ | 1.7 | 1.8 | 1.7 | 1.4 | 1.6 | 1.8 | 1.8 | 1.7 | 2.0 | 1.2 | 4.3 | 2.3 | 2.9 | 1.5 |
| Component | | | | | | | | | | | | | | |
| | Ol*** | Ol | Ol | Ol | | Ol | Ol | Ol | Ol | Ol | Ol | Ol | | Cpx |
| $SiO_2$ | 41.61 | 40.73 | 40.35 | 40.86 | | 40.84 | 41.19 | 40.91 | 40.49 | 40.20 | 40.16 | 40.84 | | 54.20 |
| $TiO_2$ | | | | | | | | | | | | | | 0.21 |
| $Al_2O_3$ | | | | | | | | | | | | | | 0.95 |
| $FeO$ | 8.81 | 9.27 | 9.52 | 9.87 | | 9.90 | 10.08 | 10.27 | 11.29 | 12.31 | 13.39 | 9.95 | | 2.74 |
| $MnO$ | 0.12 | 0.16 | 0.14 | 0.15 | | 0.20 | 0.16 | 0.17 | 0.19 | 0.17 | 0.20 | 0.15 | | 0.03 |
| $MgO$ | 49.43 | 48.89 | 48.37 | 49.24 | | 48.81 | 48.91 | 48.73 | 47.34 | 46.87 | 46.27 | 48.16 | | 17.73 |
| $CaO$ | 0.21 | 0.18 | 0.18 | 0.18 | | 0.22 | 0.20 | 0.22 | 0.21 | 0.16 | 0.16 | 0.18 | | 22.79 |
| $Na_2O$ | | | | | | | | | | | | | | 0.06 |
| $NiO$ | 0.21 | 0.16 | 0.18 | 0.18 | | 0.25 | 0.22 | 0.11 | 0.08 | 0.16 | 0.19 | 0.26 | | 0.08 |
| $Cr_2O_3$ | 0.00 | 0.05 | 0.00 | 0.04 | | 0.04 | 0.04 | 0.05 | 0.04 | 0.05 | 0.00 | 0.05 | | 0.809 |
| Total | 100.40 | 99.43 | 98.74 | 100.52 | | 100.26 | 100.80 | 100.45 | 99.64 | 99.93 | 100.37 | 99.58 | | 99.58 |
| Mg#, mol % | 90.9 | 90.4 | 90.1 | 89.9 | | 89.8 | 89.6 | 89.4 | 88.2 | 87.2 | 86.0 | 89.6 | | 92.0 |

Note: [1] FeO and [2] $Fe_2O_3$ were calculated from the total measured FeO concentration of spinel with the use of stoichiometric considerations. [3] The $Fe^{+2}/Fe^{3+}$ ratio in melt in equilibrium with spinel was calculated by the model (Maurel and Maurel, 1982). [4] The oxygen fugacity during spinel crystallization (expressed as deviation form the quartz–magnetite–fayalite buffer, in logarithmic units) was calculated by the model (Ballhaus *et al.*, 1993) at a temperature of 1200°C and a pressure of 1.0 GPa. All analyses were performed at the Vernadsky Institute of Geochemistry and Analytical Chemistry, Russian Academy of Sciences. *Grain, ** Cr-spinel inclusion, *** host mineral.

**Table 4.** Major- and trace-element composition of clinopyroxene

| Component | 1 | 2 |
|---|---|---|
| | px3/1 | px8 |
| $SiO_2$ | 54.59 | 54.84 |
| $TiO_2$ | 0.10 | 0.08 |
| $Al_2O_3$ | 1.08 | 1.05 |
| FeO | 2.69 | 2.77 |
| MnO | 0.07 | 0.08 |
| MgO | 18.09 | 17.73 |
| CaO | 22.38 | 23.19 |
| $Na_2O$ | 0.24 | 0.18 |
| $Cr_2O_3$ | 0.74 | 0.78 |
| Total | 99.98 | 100.70 |
| Mg#, mol % | 92.3 | 92.0 |
| B | 0.13 | 0.14 |
| Li | 1.78 | |
| Be | 0.005 | 0.014 |
| K | 4.5 | |
| Ti | 650 | 660 |
| Cr | | 4156 |
| Sr | 20.2 | 28.2 |
| Y | 1.96 | 1.98 |
| Zr | 0.58 | 0.90 |
| Nb | 0.14 | 0.23 |
| Ba | 0.03 | 0.14 |
| La | 0.07 | 0.11 |
| Ce | 0.37 | 0.44 |
| Nd | 0.52 | 0.69 |
| Sm | 0.27 | 0.30 |
| Eu | 0.09 | 0.11 |
| Dy | 0.43 | 0.41 |
| Er | 0.21 | 0.27 |
| Yb | 0.18 | 0.16 |
| Th | 0.016 | 0.016 |

Note: 1—Pyroxene inclusion in olivine $Fo_{88.4}$; 2—core of a clinopyroxene phenocryst. Oxides are given in wt %, elements are in ppm.

cumulates), the cooling of the magma, and the diffusion-controlled reequilibration of the crystals. None of these processes could be instantaneous. The evolution of any natural magmatic system should follow a scenario in which crystallization is associated with the partial reequilibration of preexisting crystals. In the context of our discussion, the problem is as to how closely the composition of the most magnesian minerals of avachites approximates the composition of the liquidus assemblage in the parental melt.

The effect of equilibrium crystallization on the composition of phenocrysts can be assayed by correlating the composition of the olivine and the concentrations of incompatible elements (such as Al and Ti) in the coexisting clinopyroxene (Fig. 9) or spinel. Inasmuch as the diffusion of Mg and Fe in olivine is much faster than the diffusion of Al and Ti (Jurewicz and Watson, 1988), olivine reequilibration with the melt should have led to a distortion of correlations between the compositions of pyroxene inclusions and olivine. In principle, this exactly corresponds to the situation with three pyroxene inclusions whose $Al_2O_3$ contents range from 1.1 to 1.7 wt %, which were analyzed in different crystals of olivine of practically the same composition ($Fo_{88.5}$; Fig. 9). It is reasonable to assume that olivine with an inclusion of low-Al pyroxene was originally more magnesian (~$Fo_{90}$) and was then reequilibrated with the more evolved melt. However, the analysis of correlations in Fig. 9 does not reveal any indications that avachites once contained minerals of much more magnesian composition than those present now in the rocks (for example, this could be very low-Al pyroxene with <0.8 wt % $Al_2O_3$ in olivine of "normal" composition). If the concurrent crystallization of pyroxene and olivine was preceded by the crystallization of olivine as the only liquidus phase, the parental avachite melts could be in equilibrium with more magnesian olivine than $Fo_{91}$. This olivine could either reequilibrate with the evolved melt or be simply absent from our sample. Available data do not rule out this scenario. Nevertheless, the identified composition of the earliest assemblage of olivine, pyroxene, and spinel (Table 8) most probably corresponds to the simultaneous appearance of these minerals on the liquidus, and, thus, avachite crystallization in compliance with the predominantly fractional mechanism starting at the moment of pyroxene appearance.

Liquidus assemblages of olivine, clinopyroxene, and spinel of composition close to those in avachites were also found in other moderately and highly potassic island arc series, such as those at Vanuatu (Eggins, 1993), Mexico (Carmichael, 2002), and the Solomon Islands (Ramsay *et al.*, 1984), and is typical of boninites (see, for example, Sobolev *et al.*, 1993; Portnyagin *et al.*, 1996). In Kamchatka, a liquidus assemblage of similar composition is typical of magmas in the Central Kamchatkan Depression (for example, Klyuchevskoy and Sheveluch volcanoes; Figs. 5, 7, 10). In this sense, avachites are not unique but rather present one of the most glaring example of primitive island arc basalts that form a continuous compositional series from ankaramite to high-Ca boninite and avachites somewhere in between (Fig. 11). At the same time, the composition of the liquidus minerals of avachites is unusual for magmas in southern Kamchatka and the Eastern Volcanic Front, where Avachinsky volcano is located. These magmas contain no high-Mg olivine and pyroxene, their spinel is much more aluminous, and plagioclase appeared on their liquidus quite early (see, for

example, Popolitov and Volynets, 1981). The occurrence of avachites among lavas of Avachinsky volcano suggests either unusual conditions for deep magma generation or some tectonic phenomena facilitated the eruption of these magmas at the surface.

### Composition of the Possible Parental Melt

Provisional evaluations of the composition of the parental avachite melts can be made based on (1) the composition of minerals contained in these rocks and (2) the composition of the rocks themselves. The former approach is the most accurate, because it provides direct information on the composition of the melt from which these minerals crystallized. The disadvantages of this method are also quite obvious. The distribution coefficients of elements between minerals and melts commonly strongly depend on temperature, pressure, and the concentrations of other elements in the melt (see, for example, Green, 1994), which are not known *a priori*. The other approach makes use of the composition of the rocks. This is a simple method, which can provide exhaustive information on the chemistry of the possible parental melt, received wide recognition among petrologists (see, for example, Ariskin *et al.*, 1995). The method is underlain by the assumption that the composition of the rocks is equal to that of the melts that existed in nature. This approach can be readily applied to aphyric and mildly porphyritic rocks, but if the rock contains numerous phenocrysts, as is the case with avachites, the composition of the melt should correspond, in the general case, only to the composition of the groundmass. The spatial redistribution of minerals within the crystallizing magma can result in often unsystematic variations in the proportions of these minerals in the rock, with these proportions deviating from the proportions of minerals that originally crystallized from the melt. In a marginal situation, the "groundmass" melt can be genetically independent of the crystallization of phenocryst minerals and act solely as a transporting agent, which merely entrains these minerals to the surface from the earlier cumulates. The chemical composition of these mechanical mixtures is controlled by the linear laws of mixing and can be principally different from the actual liquid lines of descent of the magma. Nevertheless, we cannot rule out the possibility that pyroxene and olivine were contained in avachites in cotectic proportions. Below we will evaluate the composition of the parental avachite melt on the basis of this principal assumption.

The Mg# of avachites varies from 73 to 82 mol %. Judging by the composition of the spinel inclusions in olivine of these rocks, the melt crystallized under oxidized conditions. The evaluations produced following the procedure in (Ballhaus *et al.*, 1993) yielded an oxygen fugacity $\Delta QFM = 1.7 \pm 0.3$ (1$\sigma$), where $\Delta QFM$ is the relative deviation of $\log_{10}(f_{O_2})$ from the QFM buffer. In magmas undersaturated with respect to ortho-

**Table 5.** Composition (wt %) of orthopyroxene phenocrysts

| Oxide | av2-3 | | #660 |
|---|---|---|---|
| | core | margin | |
| SiO$_2$ | 53.14 | 53.45 | 51.91 |
| TiO$_2$ | 0.10 | 0.14 | 0.34 |
| Al$_2$O$_3$ | 0.76 | 1.03 | 0.88 |
| FeO | 16.34 | 15.92 | 19.14 |
| MnO | 0.67 | 0.56 | 0.60 |
| MgO | 26.55 | 26.95 | 20.19 |
| CaO | 1.56 | 1.49 | 5.87 |
| Na$_2$O | 0.03 | 0.02 | 0.10 |
| Cr$_2$O$_3$ | 0.00 | 0.00 | 0.03 |
| Total | 99.15 | 99.55 | 99.06 |
| Mg# | 74.3 | 75.1 | 65.3 |

Note: Mg# = Mg/(Mg + Fe), mol %. All analyses were performed at IfM-GEOMAR, Kiel, Germany.

**Table 6.** Composition (wt %) of minerals and glass in the groundmass of avachite

| Oxide | Gl | Cpx | Pl | TMag | Ilm |
|---|---|---|---|---|---|
| | 0.15* | 0.25 | 0.55 | 0.05 | <0.01 |
| SiO$_2$ | 76.73 | 51.30 | 50.07 | 0.21 | 0.10 |
| TiO$_2$ | 1.50 | 0.63 | 0.01 | 10.05 | 45.41 |
| Al$_2$O$_3$ | 10.19 | 2.08 | 30.59 | 1.07 | 0.15 |
| FeO | 1.70 | 11.08 | 1.14 | 85.66 | 48.73 |
| MnO | 0.03 | 0.22 | 0.02 | 0.37 | 0.71 |
| MgO | 0.08 | 15.56 | 0.05 | 0.84 | 3.58 |
| CaO | 1.35 | 18.24 | 14.38 | 0.19 | 0.08 |
| Na$_2$O | 3.14 | 0.45 | 3.27 | | |
| K$_2$O | 3.39 | | 0.11 | | |
| Total | 98.11 | 99.56 | 99.65 | 98.39 | 98.75 |

Note: *Gl*—glass, *Cpx*—clinopyroxene, *Pl*—plagioclase, *TMag*—titanomagnetite, *Ilm*—ilmenite. All analyses were conducted at the Moscow State University. * Approximate volumetric phase proportions in the rock groundmass.

pyroxene, this estimate marks the maximum possible value. At this oxygen fugacity, the $Fe^{2+}/Fe^{3+}$ ratio of the melt corresponding to avachite should have been $4.0 \pm 0.5$ (1$\sigma$) (Borisov and Shapkin, 1989). The estimates made following (Maurel, 1982) suggest somewhat more reduced conditions ($Fe^{2+}/Fe^{3+} = 7.0 \pm 1.3$), which correspond to $\Delta QFM \sim 0.5$. Assuming this value as the actual degree of oxidation of the avachite melts and the $Fe^{2+}$ and Mg distribution coefficients between olivine and melt equal to 0.33 (Ford *et al.*, 1983), we arrive at the conclusions that the bulk-rock compositions of avachites could be in equilibrium with olivine of the com-

**Table 7.** Composition (wt %) of minerals in microxenoliths

| Oxide | xenolith 5 | | | xenolith 9 | | | |
|---|---|---|---|---|---|---|---|
| | *Cpx* | *Ol* | *Pl* | *Ol* | *Opx* | *Pl* | *Cpx* |
| $SiO_2$ | 53.14 | 38.67 | 53.14 | 37.66 | 53.30 | 52.33 | 51.75 |
| $TiO_2$ | 0.38 | | | | 0.55 | | 0.29 |
| $Al_2O_3$ | 1.63 | | 28.47 | | 1.31 | 28.95 | 2.41 |
| FeO | 6.78 | 17.43 | 0.87 | 23.08 | 14.86 | 1.20 | 5.55 |
| MnO | 0.27 | 0.31 | | 0.31 | 0.34 | | 0.21 |
| MgO | 17.24 | 42.60 | 0.12 | 38.24 | 26.33 | 0.26 | 16.33 |
| CaO | 20.26 | 0.20 | 12.05 | 0.18 | 2.16 | 12.36 | 22.46 |
| $Na_2O$ | 0.24 | | 4.47 | | 0.42 | 4.26 | 0.30 |
| $K_2O$ | | | 0.32 | | 0.09 | 0.17 | |
| $Cr_2O_3$ | 0.01 | 0.08 | | 0.04 | 0.33 | | 0.30 |
| Total | 99.93 | 99.28 | 99.44 | 99.51 | 99.68 | 99.51 | 99.59 |
| Mg#, *An* | 82.0 | 81.4 | 59.8 | 74.7 | 76.0 | 61.6 | 84.0 |

Note: Mg# = 100 Mg/(Mg + Fe) for olivine, clino-, and orthopyroxene, *An* = 100Ca/(Ca + Na) for plagioclase. All analyses were conducted at the Moscow State University.

**Table 8.** Composition (wt %) of the liquidus assemblage of avachites, potential parental melts, and mantle sources

| Component | 1 | 2 | 3 | 4 | 5 | 6 | 7 |
|---|---|---|---|---|---|---|---|
| | *Ol* | *Cpx* | *Spl* | AV-91 | AV-94 | TQ | MPY-87 |
| $SiO_2$ | 41.5 | 54.6 | | 52.1 | 50.5 | 45.1 | 44.6 |
| $TiO_2$ | | 0.10 | 0.35 | 0.62 | 0.5 | 0.08 | 0.16 |
| $Al_2O_3$ | | 1.08 | 9.7 | 11.9 | 10.1 | 3.2 | 4.4 |
| $FeO_{tot}$ | 8.8 | 2.7 | 22.8 | 8.4 | 8.2 | 7.7 | 9.9 |
| MnO | 0.12 | 0.07 | 0.28 | 0.2 | 0.1 | 0.14 | 0.10 |
| MgO | 49.3 | 18.1 | 12.6 | 13.1 | 18.9 | 40.2 | 37.1 |
| CaO | 0.21 | 22.4 | | 11.1 | 9.4 | 3.0 | 3.4 |
| $Na_2O$ | | 0.24 | | 1.95 | 1.63 | 0.18 | 0.39 |
| $K_2O$ | | | | 0.46 | 0.43 | | |
| $P_2O_5$ | | | | 0.14 | 0.12 | | |
| $Cr_2O_3$ | 0.05 | 0.74 | 54.3 | | | 0.45 | |
| Mg#, mol % | 90.9 | 92.3 | 59.0* | 73.6 | 80.4 | 90.3 | 87.0 |
| $CaO/Al_2O_3$ | | | | 0.93 | 0.93 | 0.93 | 0.77 |

Note: (1–3) Composition of the liquidus mineral assemblage of avachites; (4) AV-91, the evaluated parental melt of avachites in equilibrium with $Fo_{91}$; (5) AV-94, the evaluated parental melt of avachites in equilibrium with $Fo_{94}$; (6) TQ, Tinaquillo depleted lherzolite (Falloon *et al.*, 2001); (7) MPY-87, undepleted lherzolite (Falloon *et al.*, 2001); Mg# is the Mg mole fraction of spinel with regard for the $Fe^{2+}$ and $Fe^{3+}$ proportion. All analytical totals of oxides are normalized to 100 wt %.

position $Fo_{92-94}$ (Fig. 3). The most magnesian olivine in avachites has the composition $Fo_{91}$. The higher Mg# of avachites than that required to explain the olivine composition suggests excess amounts of olivine and pyroxene phenocrysts in the rocks.

Assuming that olivine and pyroxene phenocrysts are contained in avachites in cotectic proportions and the groundmass composition corresponds to the final product of the magma evolution, one can evaluate the composition of the parental melt by subtracting the average olivine and pyroxene compositions, taken in the modal proportion of these minerals, from the average composition of avachites before their equilibrium with olivine $Fo_{91}$ (Table 8, composition AV-91). The evaluated composition of the parental melt corresponds to high-Mg
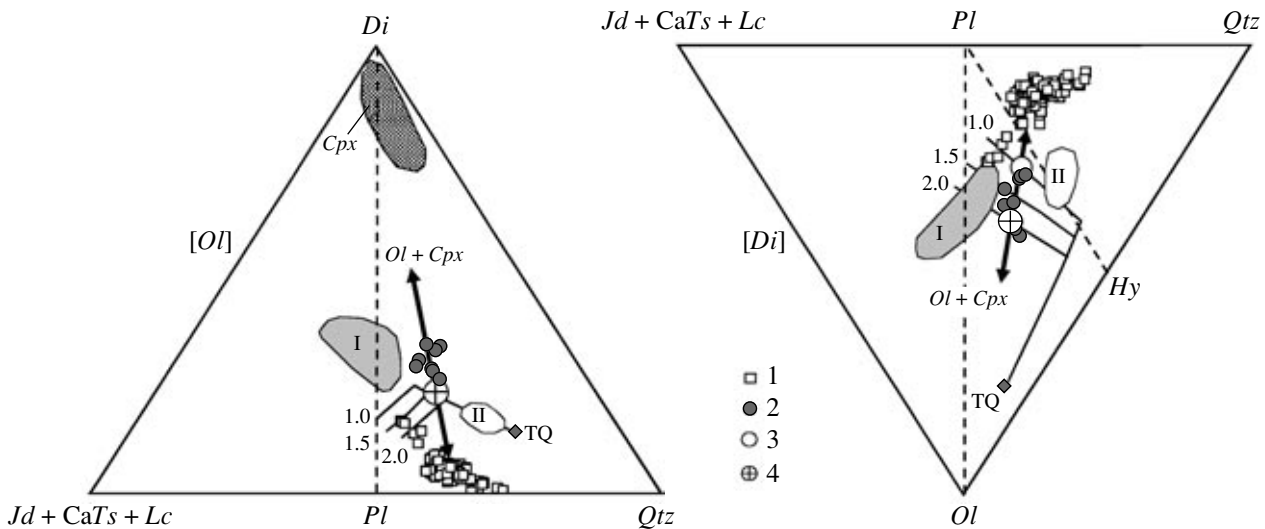
**Fig. 11.** Composition of lavas of Avachinsky volcano and their parental melts in projections in the normative olivine [*Ol*]–quartz [*Qtz*]–diopside [*Di*]–jadeite + Ca-tschermakite + leucite [*Jd* + Ca*Ts* + *Lc*] basaltic tetrahedron (Falloon and Green, 1987): (a) projection from the *Ol* apex, (b) projection from the *Di* apex.

(1) Lavas of Avachinsky volcano; (2) avachite; (3) avachite parental melt AV-91 (Table 8); (4) avachite parental melt AV-94 (Table 8).

The partial melting trajectory for the Tinaquillo peridotite (*TQ*) at 1.0, 1.5, and 2.0 GPa are shown according to (Falloon *et al.*, 2001 and references therein). Fields : I—primitive arc ankaramites, II—high-Ca boninites (Green *et al.*, 2004). The field labeled *Cpx* corresponds to the clinopyroxene composition in avachites. Heavy arrows indicate the directions of accumulation (toward the *Di* and *Ol* apices) and crystallization (toward the rocks of Avachinsky volcano) of olivine and pyroxene from parental melt AV-91 (see Table 8).

hypersthene-normative basalt (52 wt % SiO$_2$, 13 wt % MgO), whose chemistry is intermediate between those of high-Ca boninites and ankaramites (Fig. 11). This melt could be in equilibrium with clinopyroxene with Mg# ~ 92.5 mol % under a pressure of approximately 1.0 GPa and a temperature close to 1380°C (Danyushevsky *et al.*, 1996; Putirka *et al.*, 1996). The IR spectroscopic data suggest that olivine of avachites crystallized from a hydrous melt, and, hence, the initial crystallization temperatures were lower (see, for example, Falloon and Danyushevsky, 2000). Inasmuch as available data are insufficient for quantitative evaluating the H$_2$O concentration in the avachite parental melt, the estimated temperatures should be regarded as the maximum values. If high-Mg olivine (*Fo*$_{>91}$) contained in the rocks was reequilibrated with the evolved melt or was lost in the course of crystallization, then avachites could crystallize from more magnesian melts. Their composition was evaluated by simulating the fractional addition of olivine to the melt AV-91 until equilibrium was achieved with olivine of the composition *Fo*$_{94}$ (Table 8, melt AV-94).

The high Mg# of the liquidus minerals of avachites meets the requirement that their probable parental melts AV-91 and AV-94 should have been in equilibrium with mantle peridotites (Fig. 10d). The high Cr# of the liquidus spinel [Cr# = Cr/(Cr + Al) ~ 0.8] and the low concentrations of LREE, Ti, and Y testify to high degrees of mantle partial melting and to a harzburgite residue of the avachite parental melts (Arai, 1994; Jaques and Green, 1980). A potential source of these

parental magmas could be depleted peridotite, such as the Tinaquillo peridotite (Falloon *et al.*, 2001), whose composition is depleted in basaltic components somewhat more significantly than the hypothetical sources of typical basalts in oceanic rifts (for example, MPY lherzolite, Falloon *et al.*, 2001). As follows from Fig. 11, the partial melting of a source like the Tinaquillo lherzolite can give rise to melts close to AV-91 and AV-94 within the pressure range of 1–2 GPa. The residue after magma derivation should be harzburgite, as follows from the position of the melt data points to the right of the breakpoint of the mantle melting cotectics in the projection of the basaltic tetrahedron from the olivine apex. This is caused by the disappearance of clinopyroxene from the liquidus assemblage (Fig. 11). This conclusion is consistent with data on the composition of the liquidus spinel and with data on the geochemistry of the magmas.

The compositions of the parental avachite magmas assayed from the chemistries of the rocks and minerals are fairly realistic and could result from the partial melting of typical mantle peridotites. The crystallization of these melts at shallow depths could give rise to the whole spectrum of minerals composing avachites. However, some observations cannot be explained within the framework of the model expounded above. As follows from Fig. 11, parental avachite melt AV-91 should have been in equilibrium with the harzburgite mineral assemblage under the pressures of initial crystallization (close to 1.0 GPa). However, no magnesian orthopyroxene was found in the early phenocryst
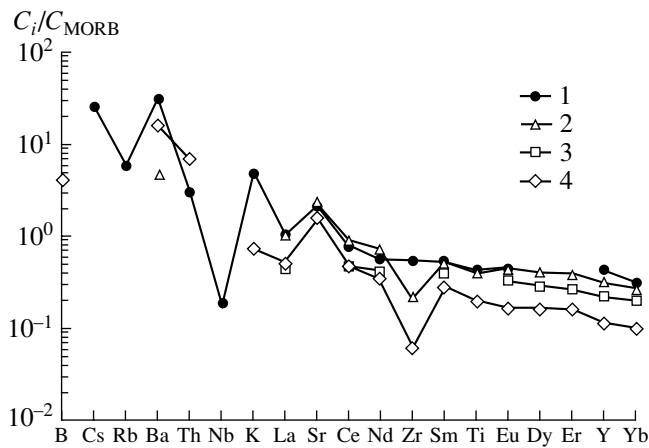
$C_i/C_{MORB}$



**Fig. 12.** Concentrations of trace elements in the avachite parental melt normalized to N-MORB (Hofmann, 1988).
(1) Calculated from the rock composition; (2–4) calculated from the composition of liquidus clinopyroxene with the use of partition coefficients of elements between pyroxene and melt: (2) after (Sobolev *et al.*, 1996), (3) (Wood and Blundy, 1997), (4) (Hart and Dunn, 1993).

assemblage of avachites, and this mineral appears on the liquidus only in much more evolved magmas. In contrast to the evaluated composition of the rocks, an orthopyroxene-undersaturated composition of the parental magmas was also inferred from the structural setting of the OH⁻ group in the olivine contained in ava-chites (see above). These facts suggest that the parental avachite melt could have a composition different from that of the rocks.

The differences between the compositions of the rocks and the actual parental melt of avachites can be explained by the multistage character of the process (Danyushevsky *et al.*, 2002), when crystals settled to form a cumulate during the slow cooling of the magma and were then brought to the surface by later magma portions. Obviously, within the framework of this model, the melt that entrained minerals of avachites could significantly differ in composition from the melt from which the phenocryst minerals crystallized, and, hence, the estimated compositions of the melts parental for the phenocrysts can be inaccurate. The composition of the parental melts can be evaluated independently by studying melt inclusions in minerals contained in the rocks, as was done in (Portnyagin *et al.*, 2005).

*Trace-Element Composition of the Parental Melt*

The concentrations of trace elements in the parental melt were assayed from the composition of the rocks and liquidus pyroxene (Table 9). In the former case, the calculations were conducted proceeding from a mass balance for the rock, olivine, and pyroxene needed to produce composition AV-91. To calculate the composition of the melt from the composition of equilibrium pyroxene, we utilized the following three sets of trace-

element partition coefficients (Table 9): (1) a set of coefficients from (Hart and Dunn, 1993), which is widely used in petrological practice; (2) coefficients calculated with the model (Wood and Blundy, 1997) on the basis of the pyroxene composition and the equilib-rium temperature and pressure; and (3) partition coeffi-cients for high-Mg (Mg# > 88 wt %) and low-alumi-nous ($Al_2O_3$ < 1.5 wt %) pyroxene obtained in (Sobolev *et al.*, 1996) by studying melt inclusions in pyroxene from high-Ca boninites from Cyprus.

Our evaluations made with the use of different approaches and different sets of partition coefficients are similar in yielding LREE contents of the parental avachite melts close to or slightly lower than the con-tents of MREE, HREE, and Y and much lower than those in N-MORB (Fig. 12). The normalized contents of B, Ba, Sr, and Th are much higher than the contents of REE of similar incompatibility and the contents of these elements in N-MORB. All models predict similar configurations of the trace-element patterns of the parental melts, whereas the estimates of the absolute concentrations of trace elements are, conversely, nota-bly different. A noteworthy close consistence (except only for Zr and Ba) was obtained by calculating the melt composition from the rock compositions and from the chemistry of clinopyroxene with the use of partition coefficient from (Sobolev *et al.*, 1996). When coeffi-cients from (Hart and Dunn, 1993) were used, the Th and Ba concentrations were reproduced realistically, whereas those of REE, Ti, Zr, and K were much lower than those evaluated based on the rock chemistries. The model in (Wood and Blundy, 1997) predicts REE con-centrations in the melt intermediate between those cal-culated from the rock compositions and with the use of coefficients from (Hart and Dunn, 1993).

The partition coefficients of trace elements between high-Ca pyroxene and melt vary in natural systems by more than one order of magnitude (Green, 1994) and strongly depend on the physicochemical parameters of crystallization and the chemistry of the clinopyroxene, for example, on its $Al_2O_3$ concentration (see, for instance, Blundy *et al.*, 1998). In this context, it is important to note that the pyroxene for which partition coefficients were determined in (Sobolev *et al.*, 1996) is the closest analogues of the pyroxene contained in avachites in terms of major-element concentrations (Fig. 7). This set of partition coefficients predicts trace-element concentrations in the avachite parental melt closely similar to the values independently calculated from the bulk-rock compositions. The good agreement of these results suggests that the estimates made by these two independent techniques can realistically enough reflect the actual composition of the avachite parental melt.

The low concentrations of moderately incompatible elements (Ti and HREE) in the avachite parental melt are consistent with the derivation of these magmas from a depleted source and/or with large degrees of partial

**Table 9.** Evaluated concentrations of trace elements (ppm) in the avachite parental melt

| Element | 1 | 2 | 3 | 4 | 5 | 6 | 7 | 8 |
|---|---|---|---|---|---|---|---|---|
| | $C_i(Cpx)$ | $D_i$(H&D) | $D_i$(W&B) | $D_i$(S) | $C_i$(H&D) | $C_i$(W&B) | $C_i$(S) | $C_i$(AV-91) |
| B | 0.14 | 0.036 | | | 3.75 | | | |
| Be | 0.01 | 0.047 | | | 0.21 | | | |
| Li | 1.8 | 0.59 | | | 3.05 | | | |
| Cs | | | | | | | | 0.23 |
| Rb | | | | | | | | 4.5 |
| Sr | 24.2 | 0.128 | | 0.091 | 189 | | 267 | 246 |
| K | 4.46 | 0.0072 | | | 620 | | | 4150 |
| Ba | 0.09 | 0.0007 | | 0.002 | 130 | | 39 | 253 |
| La | 0.09 | 0.054 | 0.063 | 0.028 | 1.7 | 1.5 | 3.3 | 3.3 |
| Ce | 0.41 | 0.086 | 0.090 | 0.046 | 4.7 | 4.6 | 8.9 | 7.7 |
| Nd | 0.61 | 0.187 | 0.15 | 0.090 | 3.2 | 3.9 | 6.8 | 5.4 |
| Sm | 0.28 | 0.291 | 0.21 | 0.16 | 1.0 | 1.4 | 1.8 | 1.8 |
| Eu | 0.10 | *0.458* | 0.23 | *0.17* | 0.22 | 0.45 | 0.61 | 0.60 |
| Tb | | | 0.25 | | | | | 0.35 |
| Dy | 0.42 | 0.442 | 0.25 | 0.18 | 1.0 | 1.7 | 2.4 | |
| Er | 0.24 | 0.387 | 0.23 | 0.16 | 0.62 | 1.0 | 1.5 | |
| Yb | 0.17 | 0.430 | 0.21 | 0.16 | 0.40 | 0.81 | 1.1 | 1.2 |
| Lu | | 0.433 | 0.20 | | | | | 0.18 |
| Y | 1.97 | 0.467 | 0.25 | 0.17 | 4.2 | 8.0 | 11.8 | 16 |
| Ti | 655 | 0.384 | | 0.19 | 1706 | | 3466 | 3660 |
| Zr | 0.74 | 0.123 | | 0.038 | 6.0 | | 19.8 | 52 |
| Nb | | 0.0077 | | | | | | 0.56 |
| Hf | | 0.256 | | | | | | 1.1 |
| Th | 0.016 | 0.014 | | | 1.15 | | | 0.50 |

Note: (1) Average composition of liquidus pyroxene in avachites; (2–4) pyroxene–melt partition coefficients of elements: (2) after (Hart and Dunn, 1993), (3) calculated by the model (Wood and Blundy, 1997) from the major-element composition of clinopyroxene at a temperature of 1300°C and a pressure of 1 GPa; (4) average partition coefficients for pyroxene from high-Ca boninite (<1.5 wt % $Al_2O_3$), after Sobolev *et al.*, 1996); (5–7) parental melt composition calculated with the use of the composition of the liquidus pyroxene from column 1 and the coefficients from column 2–4, respectively; (8) parental melt composition calculated from the compositions of rocks. Italicized numerals correspond to Eu partition coefficients obtained by interpolating data for Sm and Dy.

melting (>20%). The relative enrichment of the melt in the most incompatible elements (LREE, Th, and Ba) suggests that the avachite source had been metasomatized, before its melting, by an enriched component, which was likely related to the subduction of the Pacific Plate beneath Kamchatka.

### Parental Magma Crystallization

The concurrent crystallization of olivine and clinopyroxene from the parental melt should have resulted in a melt compositionally corresponding to the groundmass of the rock. The groundmass composition was evaluated by mass-balance calculations, proceeding from the rock composition and the petrographically assayed modal proportions of its phenocryst minerals and the compositions of these phenocrysts (Fig. 3,

Table 10). This melt differs from the typical basaltic andesites of Avachinsky volcano in having lower contents of $Al_2O_3$ and $Na_2O$ and higher concentrations of FeO and CaO. The calculated groundmass composition is in equilibrium with olivine $Fo_{80}$, which corresponds to the most ferrous olivine in this rock (Fig. 5), and clinopyroxene with Mg# ~ 78 mol % under a pressure of no more than 0.1 GPa and a temperature of ~1050°C, with the water content in the melt of no less than ~2 wt %, as was estimated by the method (Danyushevsky *et al.*, 1996). The crystallinity of parental melt AV-91 should have been close to 32% (12% olivine, 18% pyroxene, and 2% spinel) to yield the composition of the rock groundmass. Thus, avachites could be products of the polybaric (from 1.0 to <0.1 GPa) crystallization of olivine, clinopyroxene, and spinel at temperatures from ≤1380°C to 1050°C from a high-Mg basaltic melt. The

**Table 10.** Groundmass composition in avachite and typical composition of rocks of Avachinsky volcano deduced by mass-balance calculations from the composition of the avachite parental melt (wt %)

| Component | 1 | 2 | 3 | 4 | 5 | 6 | 7 | 8 |
|---|---|---|---|---|---|---|---|---|
| | AV | AV-91 | *Ol* | *Cpx* | *Spl* | GM | AB | AB–AV |
| SiO$_2$ | 51.90 | 52.1 | 40.42 | 52.42 | 0.24 | 54.94 | 55.27 | 55.54 |
| TiO$_2$ | 0.54 | 0.62 | | 0.22 | 2.38 | 0.75 | 0.88 | 0.82 |
| Al$_2$O$_3$ | 10.57 | 11.9 | | 2.05 | 10.47 | 16.09 | 18.17 | 18.35 |
| FeO$_{tot}$ | 8.23 | 8.4 | 11.42 | 5.04 | 33.60 | 8.38 | 7.39 | 8.04 |
| MnO | 0.13 | 0.2 | 0.19 | 0.16 | 0.28 | 0.11 | 0.16 | 0.15 |
| MgO | 14.11 | 13.1 | 47.72 | 17.44 | 9.96 | 5.84 | 4.60 | 4.75 |
| CaO | 11.60 | 11.1 | 0.19 | 21.42 | | 10.38 | 8.51 | 8.75 |
| Na$_2$O | 1.82 | 1.95 | | 0.19 | | 2.86 | 3.44 | 3.15 |
| K$_2$O | 0.37 | 0.46 | | | | 0.60 | 0.62 | 0.76 |
| P$_2$O$_5$ | 0.09 | 0.14 | | | | 0.15 | 0.15 | 0.23 |
| | | | | Weight proportions of phases | | | | |
| Balance 1 | 1.000 | | −0.130 | −0.240 | −0.010 | −0.620 | | |
| Balance 2 | | 1.000 | −0.119 | −0.176 | −0.019 | −0.686 | | |
| Balance 3 | | 1.000 | −0.110 | −0.267 | −0.027 | | | −0.596 |

Note: (1) Typical avachite, sample 5891 (Volynets, 1994); (2) AV-91 parental avachite melt (see Table 8); (3) average composition of olivine in avachites; (4) average composition of clinopyroxene in avachites; (5) average composition of spinel in avachites; (6) calculated groundmass composition; (7) average composition of the lavas of Avachinsky volcano (Castanella, 1988); (8) average composition of the lavas of Avachinsky volcano calculated from the composition of the avachite parental melt. Balance 1: calculation of the avachite groundmass composition, average compositions of minerals, and the measured modal proportions of these minerals in the rock (see Table 1). Balance 2: calculation of the proportions of phases crystallizing from parental AV-91 until the melt composition became equal to the composition of the rock groundmass. Balance 3: calculation of the average composition of the Avachinsky lavas from the composition of the avachite parental melt. The sum of squared discrepancies in the contents of oxides between compositions 7 and 8 is equal to 0.8.

final crystallization conditions for the groundmass assemblage (Table 6), which were calculated from the compositions of the coexisting magnetite and ilmenite (Andersen *et al.*, 1993) and likely occurred during the cooling of the lava flow, were as follows: $T = 794 \pm 10°C$ and an oxygen fugacity $\Delta QFM = 2.0 \pm 0.1$.

The differences between the groundmass compositions of avachites and the typical basaltic andesites of Avachinsky volcano indicate that either the parental melts of avachites could not be parental for the whole rock series or the crystallization conditions of avachites differed from those of the "normal" rocks of this volcano. As is demonstrated by the results of balance calculations (Table 10), the typical basaltic andesites could be generated by melt AV-91 at a higher proportion of pyroxene on the liquidus (*Ol* : *Cpx* = 1 : 2.5) than that during avachite crystallization. Hence, we cannot rule out genetic relations between avachites and the lavas of typical composition. At the same time, the primitive basalts of Avachinsky volcano (with 8–11 wt % MgO) deviate from avachites toward higher contents of normative plagioclase (Figs. 3, 11) and cannot be derived from avachites at any variations in the olivine and pyroxene proportions in the cotectics. The parental melts of these basalts were, most probably, primitive magmas of ankaramite composition (Green *et al.*,

2004), or these basalts were of hybrid genesis and were produced by the mixing of the typical Avachinsky basaltic andesite and primitive ankaramite (Fig. 11).

## CONCLUSIONS

The results of our research demonstrate that avachites are porphyritic volcanic rocks that could be generated by the crystallization of olivine ($Fo_{91–80}$), clinopyroxene (Mg# = 92.5–73 mol %), and spinel [Mg# = 18–59 mol %, Cr/(Cr + Al) = 0.82–0.55] from a parental basaltic melt (SiO$_2$ ≤ 52 wt %, MgO ~ 13 wt %) of composition intermediate between island arc ankaramite and high-Ca boninite. The IR spectroscopy of the olivine suggests that the melt contained ≥0.5 wt % H$_2$O. The high-Mg composition of avachites (14–20 wt % MgO) is explained by the accumulation of the phenocryst assemblage in the evolved (~5 wt % MgO) basaltic melt composing the rock groundmass. The minerals crystallized under pressures of 1.0–0.1 GPa, at temperatures from ≤1380°C to 1050°C, and at an oxygen fugacity $\Delta QFM = 0.5$–2.0. The parental melts of avachites were produced by high (>20%) degrees of the partial melting of a source of lherzolite composition that had been metasomatized by a component (fluid or melt) rich in LREE, Th, Ba, K, and Sr.

Some typical lavas of Avachinsky volcano can be genetically interrelated with avachites through olivine and clinopyroxene crystallization from parental melts of similar composition. The composition of the associated magnesian basalts points to the chemical heterogeneity of the primitive magmas of Avachinsky volcano and to the possible participation of magmas of ankaramite composition in the formation of Kamchatkan volcanic series. The absence of magnesian orthopyroxene from the phenocryst assemblage of avachites and the IR spectroscopy of olivine from these rocks also suggest that the minerals of avachites could crystallize from a melt undersaturated with silica, in contrast to the compositions of the rocks.

## REFERENCES

1. *Active Volcanoes in Kamchatka*, Ed. by S. A. Fedotov and Yu. P. Masurenkov (Nauka, Moscow, 1991), Vol. 1 [in Russian].

2. S. Alves, P. Schiano, F. Capmas, and C. J. Allegre, "Osmium Isotope Binary Mixing Arrays in Arc Volcanism," Earth Planet. Sci. Lett. **198**, 355–369 (2002).

3. D. J. Andersen, D. H. Lindsley, and P. M. Davidson, "QUILF: a PASCAL Program to Assess Equilibria Among Fe–Mg–Ti Oxides, Pyroxenes, Olivine, and Quartz," Computers in Geosciences **19**, 1330–1350 (1993).

4. S. Arai, "Compositional Variation of Olivine–Chromian Spinel in Mg-Rich Magmas as a Guide to Their Residual Spinel Peridotites," J. Volcanol. Geotherm. Res. **59**, 279–293 (1994).

5. A. A. Ariskin, G. S. Barmina, A. Yu. Ozerov, and R. L. Nielsen, "Genesis of High-Alumina Basalts from Klyuchevskoy Volcano," Petrologiya **3** (5), 496–521 (1995) [Petrology **3** (5), 449–472 (1995)].

6. A. I. Baikov, L. P. Anikin, and R. L. Dunin-Barkovskii, "A Find of Carbonado in Volcanics of Kamchatka," Dokl. Akad. Nauk **343** (1), 72–74 (1995).

7. C. Ballhaus, "Redox States of Lithospheric and Asthenospheric Upper Mantle," Contrib. Mineral. Petrol. **114**, 331–348 (1993).

8. I. N. Bindeman, V. V. Ponomareva, J. C. Bailey, and J. W. Valley, "Volcanic Arc of Kamchatka: A Province with High- $^{18}O$ Magma Sources and Large-Scale $^{18}O/^{16}O$ Depletion of the Upper Crust," Geochim. Cosmochim. Acta **68**, 841–865 (2004).

9. J. D. Blundy, J. A. C. Robinson, and B. J. Wood, "Heavy REE Are Compatible in Clinopyroxene on the Spinel Lherzolite Solidus," Earth Planet. Sci. Lett. **160**, 493–504 (1998).

10. A. A. Borisov and A. I. Shapkin, "A New Empirical Equation for $Fe^{2+}/Fe^{3+}$ of Natural Melts as a Function of Their Composition, Oxygen Fugacity and Temperature," Geokhimiya, No. 6, 892–897 (1989).

11. I. S. E. Carmichael, "The Andesite Aqueduct: Perspectives on the Evolution of Intermediate Magmatism in West-Central (105°–99° W) Mexico," Contrib. Mineral. Petrol. **143**, 641–663 (2002).

12. B. Castellana, Geology, Chemostratigraphy, and Petrogenesis of the Avachinskiy volcano, Kamchatka, Russia: PhD thesis. Los Angeles: University of California (1998).

13. A. J. Crawford, T. J. Falloon, and D. H. Green, in *Boninites*, Ed. by A. J. Crawford (Unwin Hyman, London, 1989), pp. 1–49.

14. L. V. Danyushevsky, A. V. Sobolev, and L. V. Dmitriev, "Estimation of the Pressure of Crystallization and $H_2O$ Content of MORB and BABB Glasses: Calibration of an Empirical Technique," Mineral. Petrol. **57**, 185–204 (1996).

15. L. V. Danyushevsky, S. Sokolov, and T. Falloon, "Melt Inclusions in Phenocrysts: Using Diffusive Re-Equilibration to Determine the Cooling Hystory of a Crystal, with Implications for the Origin of Olivine-Phyric Volcanic Rocks," J. Petrol. **43**, 1651–1671 (2002).

16. S. M. Eggins, "Origin and Differentiation of Picritic Arc Magmas, Ambae (Aoba), Vanuatu," Contrib. Mineral. Petrol. **114**, 79–100 (1993).

17. T. J. Falloon and D. H. Green, "Anhydrous Partial Melting of MORB Pyrolite and Other Peridotite Compositions at 10 Kbar: Implication for the Origin of Primitive MORB Glasses," Mineral. Petrol. **37**, 181–219 (1987).

18. T. J. Falloon and L. V. Danyushevsky, "Melting of Refractory Mantle at 1.5, 2 and 2.5 GPa under Anhydrous and $H_2O$-Undersaturated Conditions: Implications for the Petrogenesis of High-Ca Boninites and the Influence of Subduction Components on Mantle Melting," J. Petrol. **41**, 257–283 (2000).

19. T. J. Falloon, L. V. Danyushevsky, and D. H. Green, "Peridotite Melting at 1 GPa: Reversal Experiments on Partial Melt Compositions Produced by Peridotite–Basalt Sandwich Experiments," J. Petrol. **42**, 2363–2390 (2001).

20. C. E. Ford, D. G. Russel, J. A. Graven, and M. R. Fisk, "Olivine–Liquid Equilibria: Temperature, Pressure and Composition Dependence of the Crystal/Liquid Cation

Partition Coefficients for Mg, Fe$^{2+}$, Ca and Mn," J. Petrol. **24**, 256–265 (1983).

21. J. B. Gill, *Orogenic Andesites and Plate Tectonics* (Springer, Berlin-Heidelberg, 1980).

22. A. I. Gorshkov, V. A. Seliverstov, A. I. Baikov, *et al.*, "Crystal Chemistry and Genesis of Carbonado from the Melanocratic Basaltoids of Avachinsky Volcano, Kamchatka Peninsula," Geol. Rudn. Mestorozhd. **37** (1), 54–66 (1995).

23. T. H. Green, "Experimental Studies of Trace Element Partitioning Applicable to Igneous Petrogenesis—Sedona 16 Years Later," Chem. Geol. **117**, 1–36 (1994).

24. D. H. Green, M. W. Schmidt, and W. O. Hibberson, "Island-Arc Ankaramites: Primitive Melts from Fluxed Refractory Lherzolitic Mantle," J. Petrol. **45**, 391–403 (2004).

25. S. R. Hart and T. Dunn, "Experimental *Cpx*/Melt Partitioning of 24 Trace Elements," Contrib. Mineral. Petrol. **113**, 1–8 (1993).

26. K. Hirose, "Melting Experiments on Lherzolite KLB-1 under Hydrous Conditions and Generation of High-Magnesian Andesitic Melts," Geology **25**, 42–44 (1997).

27. G. Hirth and D. L. Kohlstedt, "Water in the Oceanic Upper Mantle: Implications for Rheology, Melt Extraction and the Evolution of the Lithosphere," Earth Planet. Sci. Lett. **144**, 93–108 (1996).

28. A. W. Hofmann, "Chemical Differentiation of the Earth: the Relationship Between Mantle, Continental Crust and Oceanic Crust," Earth Planet. Sci. Lett. **90**, 297–314 (1988).

29. B. V. Ivanov and G. S. Plyusnin, "Sr Isotopic Composition of Andesites from Kamchatka," Vulkanol. Seismol., No. 6, 18–25 (1988).

30. A. L. Jaques and D. H. Green, "Anhydrous Melting of Peridotite at 0–15 Kb Pressure and the Genesis of Tholeiitic Basalts," Contrib. Mineral. Petrol. **73**, 287–310 (1980).

31. E. J. Jarosewich, J. A. Nelen, and J. A. Norberg, "Reference Samples for Electron Microprobe Analysis," Geostandards Newslet. **4**, 43–47 (1980).

32. K. P. Jochum, D. P. Dingwell, A. Rocholl, *et al.*, "The Preparation and Preliminary Characterisation of Eight Geological MPI-DING Reference Glasses for *In-Situ* Microanalysis," Geostandards Newslet. **24**, 87–133 (2000).

33. J. G. Jurewicz and E. B. Watson, "Cations in Olivine. Part 2: Diffusion in Olivine Xenocrysts, with Applications to Petrology and Mineral Physics," Contrib. Mineral. Petrol. **99**, 186–210 (1988).

34. V. S. Kamenetsky, A. J. Crawford, and S. Meffre, "Factors Controlling the Chemistry of Magmatic Spinel: An Empirical Study of Associated Olivine, Cr-Spinel and Melt Inclusions from Primitive Rocks," J. Petrol. **42**, 655–671 (2001).

35. P. Kepezhinskas, F. McDermott, M. J. Defant, *et al.*, "Trace Element and Sr–Nd–Pb Isotopic Constraints on a Three-Component Model of Kamchatka Arc Petrogenesis," Geochim. Cosmochim. Acta **61**, 577–600 (1997).

36. A. B. Kersting and R. J. Arculus, "Klyuchevskoy Volcano, Kamchatka, Russia: the Role of High-Flux Recharged, Tapped, and Fractionated Magma Cham-

ber(s) in the Genesis of High-Al$_2$O$_3$ from High-MgO Basalt," J. Petrol. **35**, 1–41 (1994).

37. S. A. Khubunaya, S. O. Bogoyavlenskii, T. Yu. Novgorodtseva, and A. M. Okrugina, "Mineralogy of Magnesian Basalts as A Reflection of Their Fractionation in the Magma Chamber of Klyuchevskoy Volcano," Vulkanol. Seismol., No. 3, 46–68 (1993).

38. A. V. Koloskov, M. Yu. Puzankov, and E. S. Pirozhkova, *Ultramafic Nodules in Arc Basalts with Reference to the Problem of the Composition and Genesis of the Crust–Mantle Mixtrure in Arc Systems*, Ed. by B. V. Ivanova [in Russian].

39. F. Sh. Kutyev, B. V. Ivanov, A. A. Ovsyannikov, *et al.*, "Unusual Lavas of Avachinsky Volcano," Dokl. Akad. Nauk SSSR **255** (5), 1240–1243 (1980).

40. S. Matveev, H. S. C. O'Neill, C. Ballhaus, *et al.*, "Effect of Silica Activity on OH$^-$ IR Spectra of Olivine: Implications for Low-$a$SiO$_2$ Mantle Metasomatism," J. Petrol. **42**, 721–729 (2001).

41. S. Matveev, M. Portnyagin, C. Ballhaus, *et al.*, "FT-IR Spectrum of Magmatic Olivine asIndicator of Silica Saturation for Parental Magmas," J. Petrol. **45** (2004).

42. C. Maurel and P. Maurel, "Etude Experimentale de Equilibre Fe$^{2+}$–Fe$^{3+}$ dans les Spinelles Chromifieres et les Liquides Silicates Basiques Coexistants, a 1 Atm," C. R. L'Academie Sci., Paris **295**, 209–212 (1982).

43. N. L. Mironov, M. V. Portnyagin, P. Yu. Plechov, and S. A. Khubunaya, "Final Stages of Magma Evolution in Klyuchevskoy Volcano, Kamchatka: Evidence from Melt Inclusions in Minerals of High-Alumina Basalts," Petrologiya **9** (1), 51–69 (2001) [Petrology **9** (1), 46–62 (2001)].

44. B. O. Mysen and A. L. Boettcher, "Melting of a Hydrous Mantle, II. Geochemistry of Crystals Formed by Anatexis of Mantle Peridotite at High Pressures and High Temperatures as a Function of Controlled Activities of Water, Hydrogen and Carbon Dioxide," J. Petrol. **16**, 549–593 (1975).

45. A. Y. Ozerov, "The Evolution of High-Alumina Basalts of the Klyuchevskoy Volcano, Kamchatka, Russia, Based on Microprobe Analyses of Mineral Inclusions," J. Volcanol. Geotherm. Res. **95**, 65–79 (2000).

46. F. Pineau, M. P. Semet, N. Grassineau, *et al.*, "The Genesis of the Stable Isotope (O, H) Record in Arc Magmas: the Kamchatka's Case," Chem. Geol. **135**, 93–124 (1999).

47. E. I. Popolitov and O. N. Volynets, *Geochemistry of Quaternary Volcanism of the Kurile-Kamchatka Island Arc and Some Petrogenetic Aspects*, Ed. by L.V. Tauson (Nauka, Novosibirsk, 1981) [in Russian].

48. M. V. Portnyagin, N. L. Mironov, S. V. Matveev, and P. Yu. Plechov, "Petrology of Avachites, High-Mg Basalts of Avachinsky Volcano, Kamchatka: II. Melt Inclusions in Olivine," Petrologiya (2005) (in press).

49. M. V. Portnyagin, R. Magakyan, and Kh.-U. Shminke, "Geochemical Variability of Boninite Magmas: Evidence from Magmatic Inclusions in Highly Magnesian Olivine of Southwestern Cyprus," Petrologiya **4** (3), 250–265 (1996) [Petrology **4** (3), 231–246].

50. K. Putirka, M. Johnson, R. Kinzler, *et al.*, "Thermobarometry of Mafic Igneous Rocks Based on Cli-

nopyroxene–Liquid Equilibria, 0–30 Kbar," Contrib. Mineral. Petrol. **123**, 92–108 (1996).

51. W. R. H. Ramsay, A. J. Crawford, and J. D. Foden, "Field Setting, Mineralogy, Chemistry and Genesis of Arc Picrites, New Georgia, Solomon Islands," Contrib. Mineral. Petrol. **88**, 386–402 (1984).

52. A. B. E. Rocholl, K. Simon, K. P. Jochum, *et al.*, "Chemical Characterization of NIST Silicate Glass Certified Reference Material SRM 610 by ICP-MS, TIMS, LIMS, SSMS, INAA, AAS and PIXE," Geostandards **21**, 101–114 (1997).

53. S. A. Shcheka, N. A. Kurentsova, and O. N. Volynets, in *Typomorphism of Rock-Forming Minerals* (DVGI DVO AN SSSR, Vladivostok, 1978), pp. 5–41 [in Russian].

54. A. V. Sobolev and L. V. Danyushevsky, "Petrology and Geochemistry of Boninites from the North Termination of the Tonga Trench: Constraints on the Generation Conditions of Primary High-Ca Boninite Magmas," J. Petrol. **35**, 1183–1211 (1994).

55. A. V. Sobolev, "Melt Inclusions in Minerals as a Source of Principal Petrological Information," Petrologiya **4** (3), 228–239 (1996) [Petrology **4** (3), 209–220].

56. A. V. Sobolev, A. A. Migdisov, and M. V. Portnyagin, "Incompatible Element Partition between Clinopyroxene an Basalt Liquid Revealed by the Study of Melt Inclusions in Minerals from Troodos Lavas, Cyprus," Petrologiya **4** (3), 326–336 (1996) [Petrology **4** (3), 307–317].

57. A. V. Sobolev, M. V. Portnyagin, L. V. Dmitriev, *et al.*, "Petrology of Ultramafic Lavas and Related Rocks of the Troodos Massif, Cyprus," Petrologiya **1** (4), 379–412 (1993).

58. S.-S. Sun and W. F. McDonough, "Chemical and Isotopic Systematics of Oceanic Basalts: Implications for Mantle Composition and Processes," in *Magmatism in the Ocean Basins*, Ed. by A. D. Saunders and M. J. Norry (Geological Society Special Publication, London, 1989), Vol. 42, pp. 313–345.

59. L. Tolstykh, V. B. Naumov, A. D. Babanskii, *et al.*, "Chemical Composition, Volatile Components, and Trace Elements in Andesite Magmas of the Kurile-Kamchatka Region," Petrologiya **11** (5), 451–470 (2003) [Petrology **11** (5), 407–425 (2003)].

60. O. N. Volynets, "Geochemical Types, Petrology, and Genesis of the Late Cenozoic Volcanic Rocks from the Kurile–Kamchatka Island-Arc System," Int. Geol. Rev. **36**, 373–403 (1994).

61. N. Volynets, A. D. Babanskii, and Yu. V. Gol'tsman, "Variation in Isotopic and Trace-Element Composition of Lavas from Volcanoes of Northern Group, Kamchatka, in relation to Specific Features of Subduction," Geokhimiya, No. 10, 1067–1083 (2000) [Geochem. Int. **38** (10), 974–989 (2000)].

62. O. N. Volynets, V. V. Ponomareva, and A. D. Babanskii, "Magnesian Basalts of Sheveluch Andesite Volcano, Kamchatka," Petrologiya **5** (2), 206–221 (1997) [Petrology **5** (2), 183–196].

63. B. J. Wood and J. D. Blundy, "A Predictive Model for Rare Earth Element Partitioning between Clinopyroxene and Anhydrous Silicate Melt," Contrib. Mineral. Petrol. **129**, 166–181 (1997).

64. G. M. Yogodzinsky and P. B. Kelemen, "Slab Melting in the Aleutians: Implications of an Ion Probe Study of Clinopyroxene in Primitive Adakite and Basalt," Earth Planet. Sci. Lett. **158**, 53–65 (1998).

65. A. N. Zavaritskii, *Avachinsky Volcano in Kamchatka and Its State in the Summer of 1931* in *Trudy TsNIGRI* (Moscow, 1935), No. 35 [in Russian].